UNCLASSIFIED

## AD NUMBER

AD487353

## NEW LIMITATION CHANGE

TO

Approved for public release, distribution unlimited

FROM

Distribution authorized to DoD only; Administrative/Operational use; 7 Jul 1966. Other requests shall be referred to Naval Ordnance Lab, White Oak MD .

## AUTHORITY

USNSWC ltr, 7 Oct 1974

THIS PAGE IS UNCLASSIFIED

Best Available Copy

NOLTR 66-87

487355

# THE SMALL SCALE GAP TEST: CALIBRATION AND COMPARISON WITH THE LARGE SCALE GAP TEST

Best Available Copy

NOL

7 JULY 1966

UNITED STATES NAVAL ORDNANCE LABORATORY, WHITE OAK, MARYLAND

NOLTR 66-87

This document is subject to special export controls and each transmittal to foreign governments may be made only with prior approval of NOL.

487355

Best Available Copy

(2)

# REPRODUCTION QUALITY NOTICE

This document is the best quality available. The copy furnished to DTIC contained pages that may have the following quality problems:

- Pages smaller or larger than normal.
- Pages with background color or light colored printing.
- Pages with small type or poor printing; and or
- Pages with continuous tone material or color photographs.

Due to various output media available these conditions may or may not cause poor legibility in the microfiche or hardcopy output you receive.

☐ If this block is checked, the copy furnished to DTIC contained pages with color printing, that when reproduced in Black and White, may change detail of the original copy.

# THE SMALL SCALE GAP TEST: CALIBRATION AND COMPARISON WITH THE LARGE SCALE GAP TEST

By

Donna Price and T. P. Liddiard, Jr.

ABSTRACT: The calibration of the small scale gap test (SSGT) is reported. It covers the ranges of 5 to 90 kbar in shock pressure and 2 to 20 mm in gap thickness of polymethyl methacrylate and can be simply extrapolated beyond these ranges.

Comparison of the shock sensitivities measured in the SSGT with those obtained in the large scale gap test showed quantitative correlation for explosives tested at porosity ≥ 10%. Differences at lower porosities are described and discussed.

ADVANCED CHEMISTRY DIVISION
CHEMISTRY RESEARCH DEPARTMENT
EXPLOSION DYNAMICS DIVISION
EXPLOSIONS RESEARCH DEPARTMENT
U. S. NAVAL ORDNANCE LABORATORY
WHITE OAK, MARYLAND

Best Available Copy

Best Available Copy



The work described in this report was carried out under Task Numbers RMMP 22-149-F009-06-11 Prob 000 (Propellant and Ingredient Sensitivity) and RMMO 62-058/212-1/F008-08-11 Prob 4 (Study of Explosive Properties).

This report describes the calibration (pressure vs gap length) of the small scale gap test and a comparison of the results obtained in this test with those obtained in the large scale gap test. The information contained herein is of considerable importance to the study of explosive and propellant sensitivity.

J. A. DARE
Captain, USN
Commander

J. E. ABLARD
By direction

Best Available Copy

TABLE OF CONTENTS

| | Page |
|---|---|
| INTRODUCTION | 1 |
| CALIBRATION | 1 |
| Procedure | 1 |
| Charge Systems Used in Calibration | 3 |
| Measurement of PMMA Surface Velocity | 4 |
| Determination of Pressure | 6 |
| Arbitrary Units | 12 |
| COMPARISON OF TEST VALUES OF SSGT WITH THOSE OF LSGT | 16 |
| Subcritical Behavior of NQ | 17 |
| Particle Size Effect on Measured Sensitivity | 22 |
| Apparent Reversals in Sensitivity Ratings | 23 |
| Correlation between Small and Large Scale Test Results | 28 |
| SUMMARY | 32 |
| ACKNOWLEDGMENT | 32 |
| REFERENCES & NOTES | 33 |
| APPENDIX A, SUPPLEMENTARY DATA | 35 |
| APPENDIX B, MEASUREMENT OF SHOCK VELOCITY | 45 |

TABLES

| Table | | |
|---|---|---|
| 1 | Measured Free Surface Velocities in SSGT Systems | 9 |
| 2 | Calibration Data for SSGT | 14 |

Best Available Copy



TABLES CONT.


| Table | | Page |
|---|---|---|
| 3 | Zero Gap Output for High Bulk Density Nitroguanidine (X446) | 20 |
| 4 | Comparison of LSGT and SSGT Results at Same % TMD | 30 |
| A1 | Hugoniot Data for PMMA and Calibration Data for LSGT | 36 |
| A2 | Data Obtained with LSGT | 37-38 |
| A3 | Data Obtained with SSGT | 39-41 |
| A4 | Ionization Probe Measurements on NQ in SSGT Configuration | 42 |
| B1 | Shock Velocity as a Function of Distance | 46 |


ILLUSTRATIONS


| Figure | Title | |
|---|---|---|
| 1 | The Complete SSGT Setup | 2 |
| 2 | Jacobs Framing Camera Sequence of Record 212 | 5 |
| 3 | Foil Trajectories from Record 220 | 7 |
| 4 | Jacobs Framing Camera Sequence of Record 217 | 8 |
| 5 | Variation of Free Surface Velocity of PMMA with Gap Thickness in SSGT | 10 |
| 6 | PMMA Hugoniot Data Obtained in Calibration of LSGT | 10 |
| 7 | Calibration Data for SSGT | 11 |
| 8 | Extrapolation of SSGT Calibration Data to Zero Gap | 13 |
| 9 | Extrapolation of LSGT Calibration Data to Zero Gap | 15 |
| 10 | Shock Sensitivity as a Function of Loading Density, LSGT | 18 |

Best Available Copy

ILLUSTRATIONS CONT.


| Figure | Title | Page |
|---|---|---|
| 11 | Shock Sensitivity as a Function of Loading Density, SSGT | 19 |
| 12 | Output (Dent/$\rho_o$) at Zero Gap for Two Nitroguanidines and Tetryl, SSGT | 21 |
| 13 | Effect of Particle Size on Shock Sensitivity of Tetryl | 21 |
| 14 | Apparent Reversal of Tetryl Sensitivity with Change in Test from Large to Small Scale | 24 |
| 15 | Example of Fictitious Sensitivity Reversal Using SSGT Results | 26 |
| 16 | Comparison of SSGT Results for Several Explosives | 27 |
| 17 | Comparison of Data from LSGT with those from SSGT up to 60 kbar in Latter | 29 |
| 18 | Correlation of SSGT and LSGT Values | 31 |
| A1 | Charge Assembly and Dimensions for NOL Standardized Gap Test, LSGT | 43 |
| A2 | Conversion of SSGT Results from Arbitrary Units to $P_g$ (kbar) | 44 |
| B1 | Shock Velocity (U) vs Distance (X) in PMMA in SSGT (X scale factor is five) | 47 |
| B2 | PMMA Hugoniot Data Obtained in Calibration of SSGT | 48 |

Best Available Copy

# The Small Scale Gap Test: Calibration and Comparison with the Large Scale Gap Test

## INTRODUCTION

The small scale gap test (SSGT) is a conventional gap or shock sensitivity test carried out in small dimensions (5 mm diam) under heavy confinement (10 mm thick brass wall). The SSGT has been extensively used to estimate shock sensitivity by testing small samples of explosive and also to determine the reliability of various fuze trains. Although it has been a useful tool, particularly since its standardization[1], interpretation of its results has been restricted by lack of a calibration and by unexplained reversals of explosives ratings when the testing is carried out on a large scale rather than a small scale test. It is the purpose of this work to remove both of these restrictions and thereby enhance the usefulness of the test.

Calibration of the donor/gap system, here reported, permits the direct interpretation of the measured 50% gap (attenuator thickness) in terms of the shock strength or amplitude. Hence the critical initiating stimulus is now given as shock stress at the end of the gap instead of in the completely arbitrary units hitherto employed.

We also report the comparison of SSGT results with those from the standardized large scale gap test[2] (LSGT) for a number of different explosives. Such comparisons outline conditions under which a good correlation exists between the two sets of results. But, in addition, the study clearly reveals other conditions under which rating reversals are to be expected.

## CALIBRATION

### Procedure

The standardized SSGT is shown in Fig. 1. The donor is RDX and the attenuator or gap material is polymethyl methacrylate (PMMA). Although the manufacturing tolerance for the donor density is 1.56 ± 0.03 g/cc, the 22 donors used for the calibration had a mean $\rho_0$ = 1.58 g/cc. Their $\rho_0$ values ranged ± 0.02 g/cc from the mean and the standard deviation was 0.006 g/cc. In shock sensitivity testing, the gap length or thickness is varied in a Bruceton type test. The 50% functional value is thus found; it is that length of attenuator with which a

Best Available Copy

# BLANK PAGE

Best Available Copy

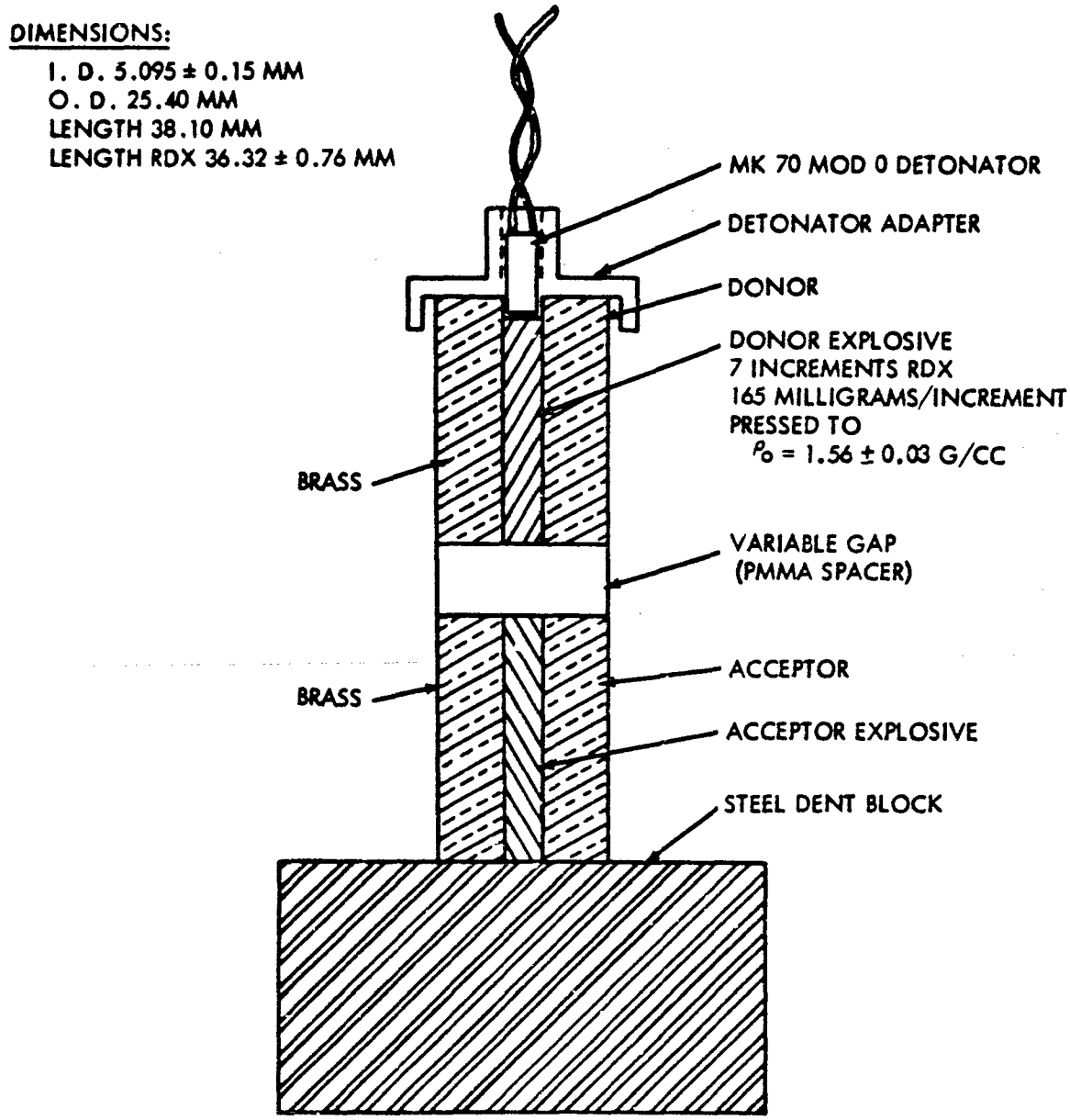


FIG. 1 THE COMPLETE SSGT SETUP

positive result* is obtained in 50% of the trials. In general, the 50% gap is that length of attenuator which permits transmission of the critical pressure required to initiate the acceptor to detonation.

Calibration of this test consists of determining the peak shock pressure (P) as a function of the distance (X) the shock has traveled along the axis of the PMMA cylindrical gap. The calibration procedure is that described in Ref. 2. Basically it consists of measuring, in the PMMA, the shock velocity (U) and free surface velocity ($u_{fs}$), each as a function of X. From the approximation

$$u_{fs} = 2\,u \tag{1}$$

the particle velocity (u) as a function of X is obtained. The desired relation, P vs X, is obtained through the hydrodynamic equation

$$P = \rho_o\,U\,u \tag{2}$$

where $\rho_o$ is the initial density of the PMMA.

Charge Systems Used in Calibration

In making the calibration, the detonator/donor/gap system of Fig. 1 was used with the acceptor and witness block omitted. However, a larger system was necessary to measure accurately the shock velocity in the PMMA. For this purpose a linearly scaled model of the donor/gap arrangement of Fig. 1 was used; the scale factor was 5.

The same type of detonator, the EX 7 Mod 0**, was used in both the actual SSGT and scaled (5x) systems. As Fig. 1 shows, the donor explosive column does not completely fill its container in the SSGT. No analogous space was left at the detonator end of the donor in the larger system. (The subsequent experiments showed that the small increase in the amount of RDX had no significant effect on the calibration.) The loading density of the RDX was within the manufacturing tolerance set for donor density. The 10 large donors (5x) had a mean value $\rho_o$ = 1.56 g/cc, $\sigma$ = 0.001g/cc.

---

*Criterion of a positive result for this test is that the depth of dent in the steel witness block be equal to or greater than half that obtained with the same acceptor shocked at zero gap.

**This is identical in explosive content to the Mark 70 service detonator, but it contains a larger diameter bridgewire for increased handling safety in the laboratory.

## Measurement of PMMA Surface Velocity

It has been found[2] that the PMMA particle velocity is a much more sensitive function of pressure than the shock velocity, particularly at low pressures. (See Table A1. For a pressure change from 18 to 5 kbar, U decreases only 10% whereas u decreases by 68%.) Consequently the free surface velocity is the more important of the two experimental measurements for calibration.

The foil method reported in Ref. 2 was used here to obtain a true surface velocity, i.e., one unretarded by the structural strength of the PMMA. Foils of 0.025 mm-thick annealed brass were chosen for this work because they were superior to the other materials previously tested in flatness (no curl) of the discs punched from flat sheet stock. They also showed good planar contact when mounted on the PMMA surface with a very thin layer of silicone grease.

As Fig. 1 shows, the donor explosive has a diameter of only 5.10 mm. The practical lower limit of foil disc diameter is about 2 mm, both from the standpoint of camera resolution and ease of preparing and mounting the disc. Hence a brass foil disc of this diameter was mounted on the center of the free surface of the PMMA in the donor/gap system of Fig. 1. Upon firing the donor, the motion of the foil was followed by either a framing or a smear camera.

Because of the very small dimensions of Fig. 1, there was a question of whether any foil in that system could be driven with the full initial velocity of the PMMA surface. To answer this question, surface velocity measurements were also carried out on the system scaled up by five. (Neither foil thickness nor foil diameter were scaled; the disc diameter used here was 3 mm). As we will show below, the two sets of $u_{fs}$ measurements scaled very well. We conclude therefore that the dimensions selected for the foils and the resultant foil performance were in an optimal range.

Fig. 2 shows the Jacobs framing camera sequence of two SSGT calibration setups fired together (Record 212 of Table 1). At the left the PMMA cylinder (gap) is 20.3 mm long and at the right it is 25.4 mm long. Backlighting in this example was provided by an exploding wire light source. A large lens placed in front of the light source was used to bring slightly convergent light rays into the front lens of the camera. (Most of the framing camera shots were made by diffuse reflected backlighting produced by the light of an argon explosive flash lamp shining on a white cardboard placed behind the subject.) The time between the frames shown here is 6.53 μsec, six frames actually having been taken in this interval. The brass foil is

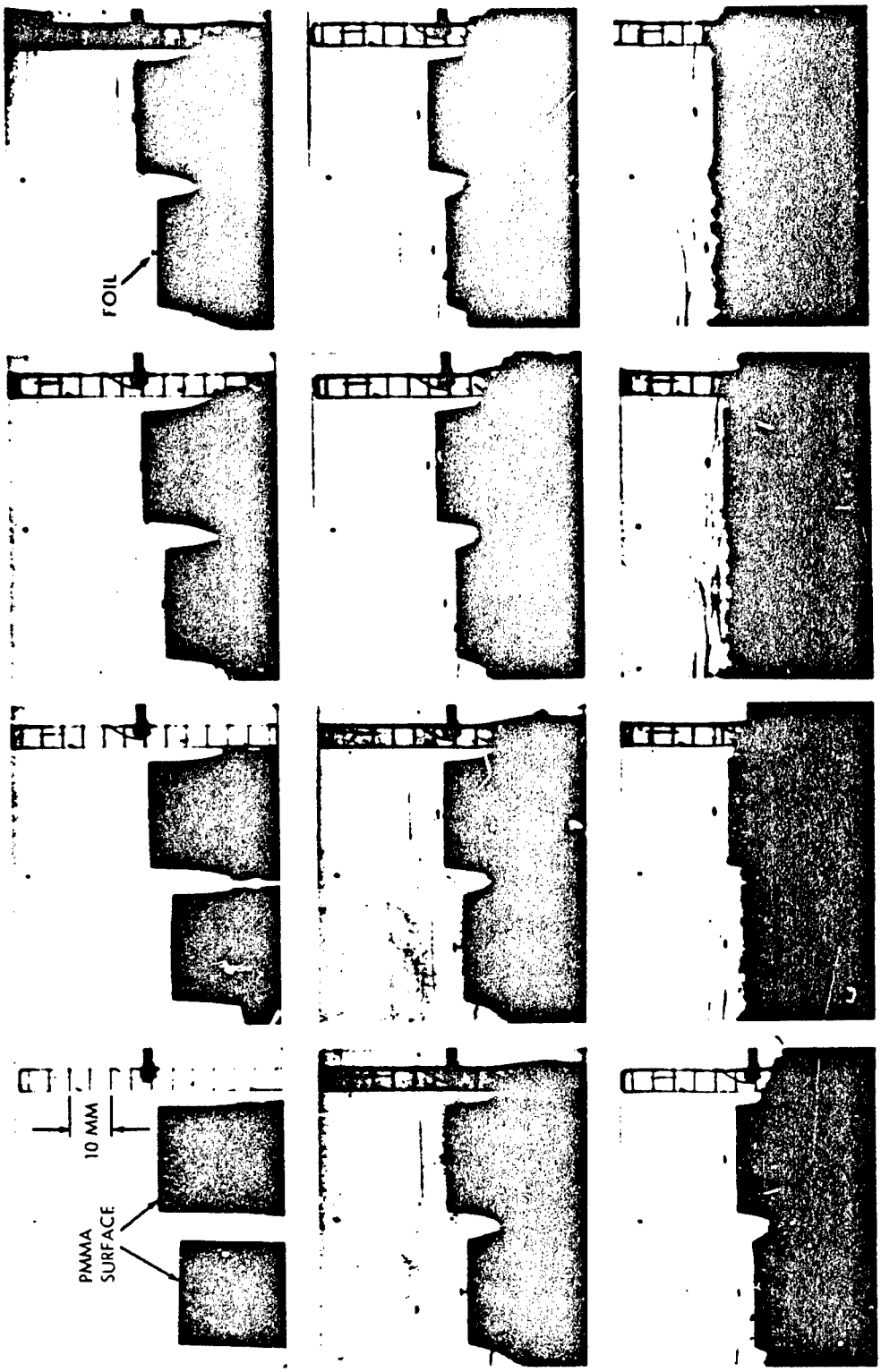


FIG. 2 JACOBS FRAMING CAMERA SEQUENCE OF RECORD 212

PMMA CYLINDERS OF 25.4MM DIAMETER, HEIGHTS ARE 20.3 AND 25.4MM, FOIL DIAMETER 2MM, INTERFRAME TIME 6.53 μSEC.

shown leaving the surface of each PMMA cylinder. No detectable retardation of the foils was noted over 30 mm or so of travel. Typical plots of foil displacements (S) vs time (t) are shown in Fig. 3 (Record 220).

For PMMA thicknesses of less than 5.08 mm (or 25.4 mm in the 5x model), the foils do not separate cleanly from the PMMA surface. Accelerating fragments of spalled PMMA partially obscure the motion of the foil. Even at a gap of 10.16 mm (or 50.8 mm, 5x model) PMMA fragments can be observed overtaking the foil. This is shown in Fig. 4 containing a sequence from Record 217.

Because of the obscuring of the foils when small gaps were used, no values of $u_{fs}$ could be measured for gaps less than 2.5 mm (12.5 mm, 5x model). This condition limits the upper range of the calibration to about 90 kbar, as will be seen.

Table 1 contains the measured foil velocity as a function of gap thickness. These data are plotted in Fig. 5. Since data on duplicate shots differ insignificantly, only the average values of duplicates are plotted.

## Determination of Pressure

Although some measurements of U vs X were made on the scaled-up model, this was done to support the consistency of the present work, not in the expectation that they could yield a U vs u relationship better than that already obtained for PMMA during the extensive work reported in Ref. 2. The current shock velocity data are reported in Appendix B, but the U vs u relation of Ref. 2 was used to convert the surface velocity data of Table 1 into the corresponding gap pressure ($P_g$).

Fig. 6 shows the Hugoniot curve for PMMA, and Table A1 contains the corresponding data from Ref. 2. They have been used, as already indicated in Table 1, to compute the listed pressures which correspond to the measured free surface velocities.

In Fig. 7 these data have been plotted as log P vs log X. They fall remarkably well on a straight line with the equation

$$\log P = 2.49 - 1.40 \log X \qquad (3)$$

where units of P and X are kbar and mm, respectively.

Eqn. (3) can be rewritten as

$$P = 309\ X^{-1.40} \qquad (4)$$

Best Available Copy

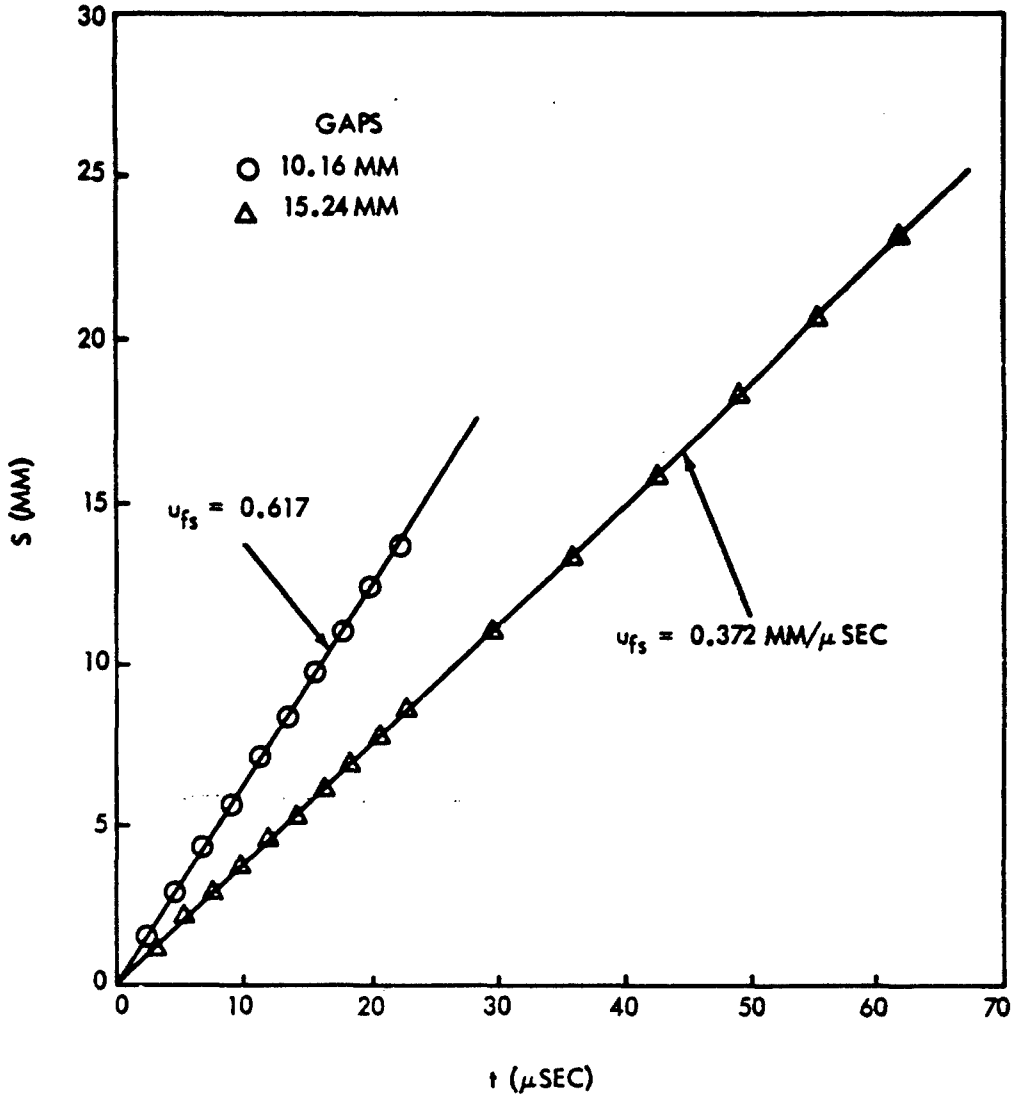


FIG. 3 FOIL TRAJECTORIES, RECORD 220

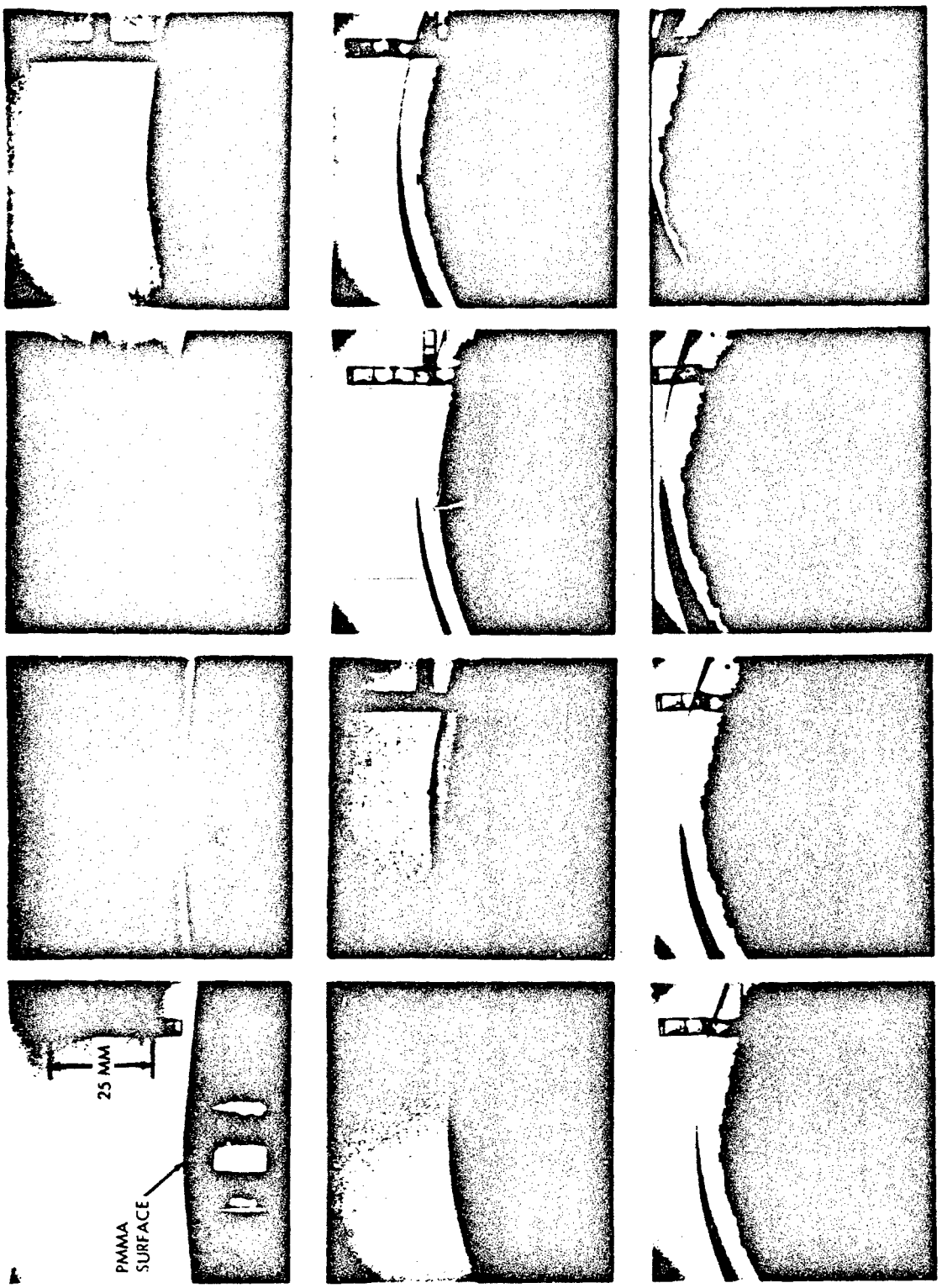


FIG. 4 JACOBS FRAMING CAMERA SEQUENCE OF RECORD 217 ILLUSTRATING SPALL OVERTAKING FOIL.

EXPERIMENTAL DETAILS: MODEL SYSTEM 5X SSGT, FOIL DIAMETER 3MM. THE FREE END OF PMMA CYLINDER (127MM DIAM, 50.8MM HIGH) HAS BEEN BEVELLED 5° TO LEAVE A PLATFORM OF 10MM DIAMETER AT CENTER. BACKLIGHTING BY THE DIFFUSE REFLECTED LIGHT OF AN EXPLOSIVE FLASHLAMP. INTERFRAME TIME: 6.53 $\mu$ SEC. FOIL OBSCURED BY PMMA SURFACE IN LAST THREE FRAMES.

TABLE 1

Measured Free Surface Velocities in SSGT Systems

| | Record No. | Gap Length X(mm) | Velocities (mm/μsec) Foil $u_{fs}$ | Particle u | Shock $U^c$ | Pressure $P_g{}^d$ kbar |
|---|---|---|---|---|---|---|
| Actual Size SSGT donor/gap | 214[a] | 2.54 | 2.73-3.02 | 1.36-1.51 | 4.76-4.99 | 76.7-88.9 |
| | 249 | 3.61 | 2.05 | 1.025 | 4.22 | 51.0 |
| | 249 | 3.62 | 2.04 | 1.020 | 4.21 | 50.7 |
| | 214[a] | 5.08 | 1.44 | 0.720 | 3.74 | 31.8 |
| | 213 | 7.62 | 0.890 | 0.445 | 3.40 | 17.9 |
| | 213 | 10.16 | 0.615 | 0.308 | 3.26 | 11.9 |
| | 220 | 10.16 | 0.617 | 0.308 | 3.26 | 11.9 |
| | 220 | 15.24 | 0.372 | 0.186 | 3.14 | 6.9 |
| | 209 | 20.32 | 0.243 | 0.122 | (3.08)[e] | (4.4) |
| | 212 | 20.32 | 0.228 | 0.114 | (3.07) | (4.1) |
| | 212 | 25.40 | 0.179 | 0.090 | (3.04) | (3.2) |
| Model 5X Size | | Gap/5 | | | | |
| | 215 | 5.08 | 1.45 | 0.725 | 3.75 | 32.1 |
| | 217 | 10.16 | 0.625 | 0.312 | 3.26 | 12.0 |
| | 218 | 20.32 | 0.245 | 0.122 | (3.08) | (4.4) |
| | 222[b] | 25.42 | 0.193 | 0.096 | (3.05) | (3.5) |
| | 223[b] | 25.40 | 0.182 | 0.091 | (3.04) | (3.3) |
| | 242[b] | 26.38 | 0.194 | 0.097 | (3.05) | (3.5) |
| | 243[b] | 26.38 | 0.190 | 0.095 | (3.05) | (3.4) |

a) Duplicate shots made with two foils, the extra one covering entire PMMA surface. These records could not be read.
b) Smear camera records; all others are from the Jacobs framing camera. In shots 222 and 223 PMMA was a 127-mm long cylinder with parallel observation flats machined on each side; in shots 242 and 243, PMMA was a 132-mm long block with cross section of 100 x 100 mm. The foil traces had small slopes and the velocities obtained are considered less reliable than those measured with the framing camera.
c) Read from Fig. 6.
d) Computed from $P_g = 11.8\ U\ u$. The PMMA density ranged from 1.18 to 1.19 g/cc.
e) Figures in parentheses obtained by extrapolation of Fig. 6.





Best Available Copy

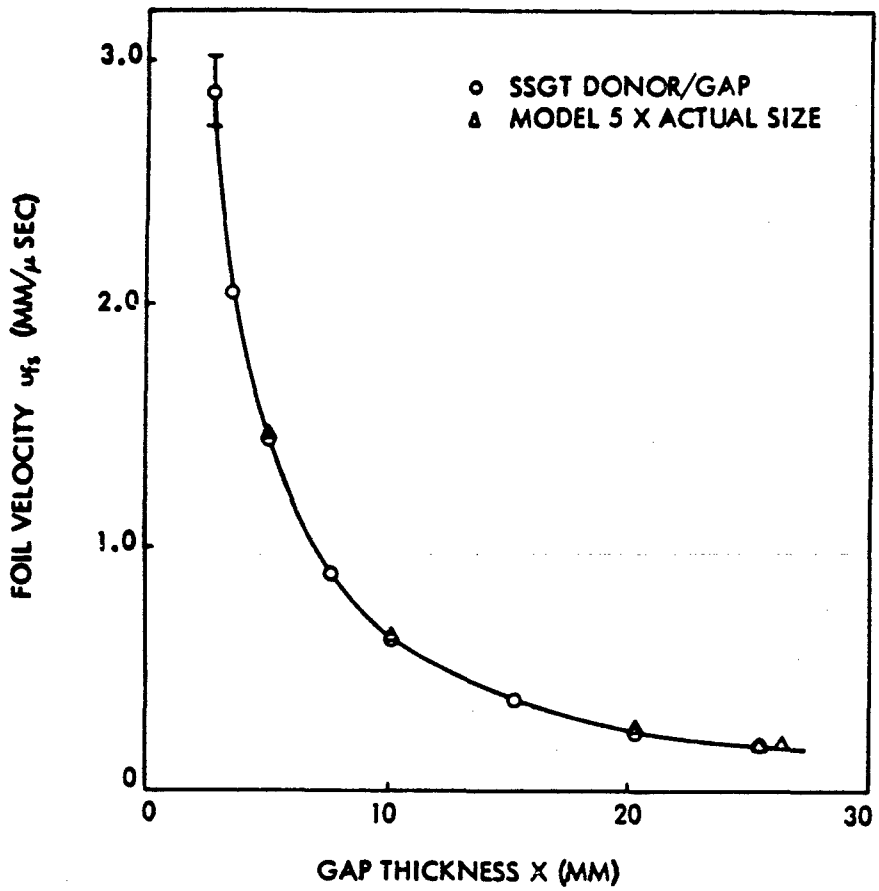


FIG. 5 VARIATION OF FREE SURFACE VELOCITY OF PMMA WITH GAP THICKNESS IN SSGT

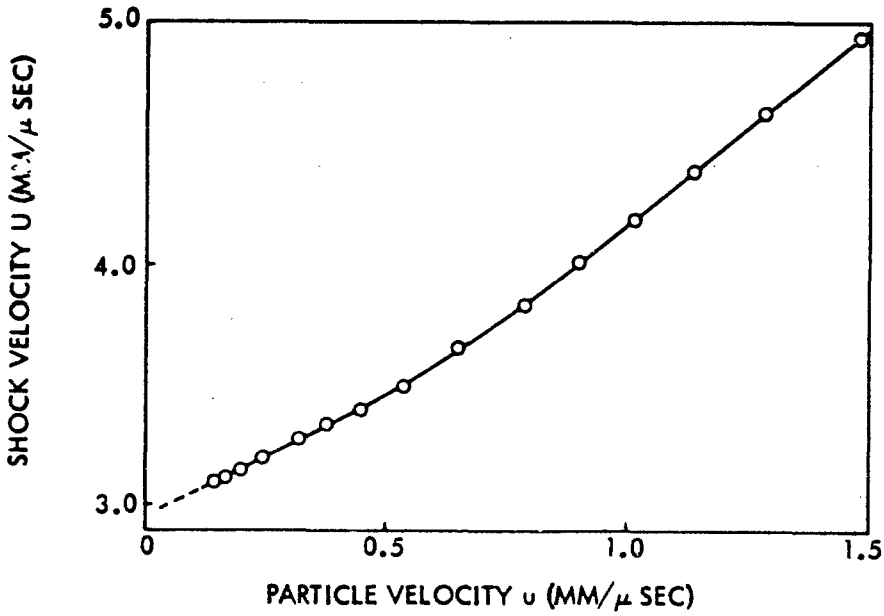


FIG. 6 PMMA HUGONIOT DATA OBTAINED IN CALIBRATION OF LSGT[2]

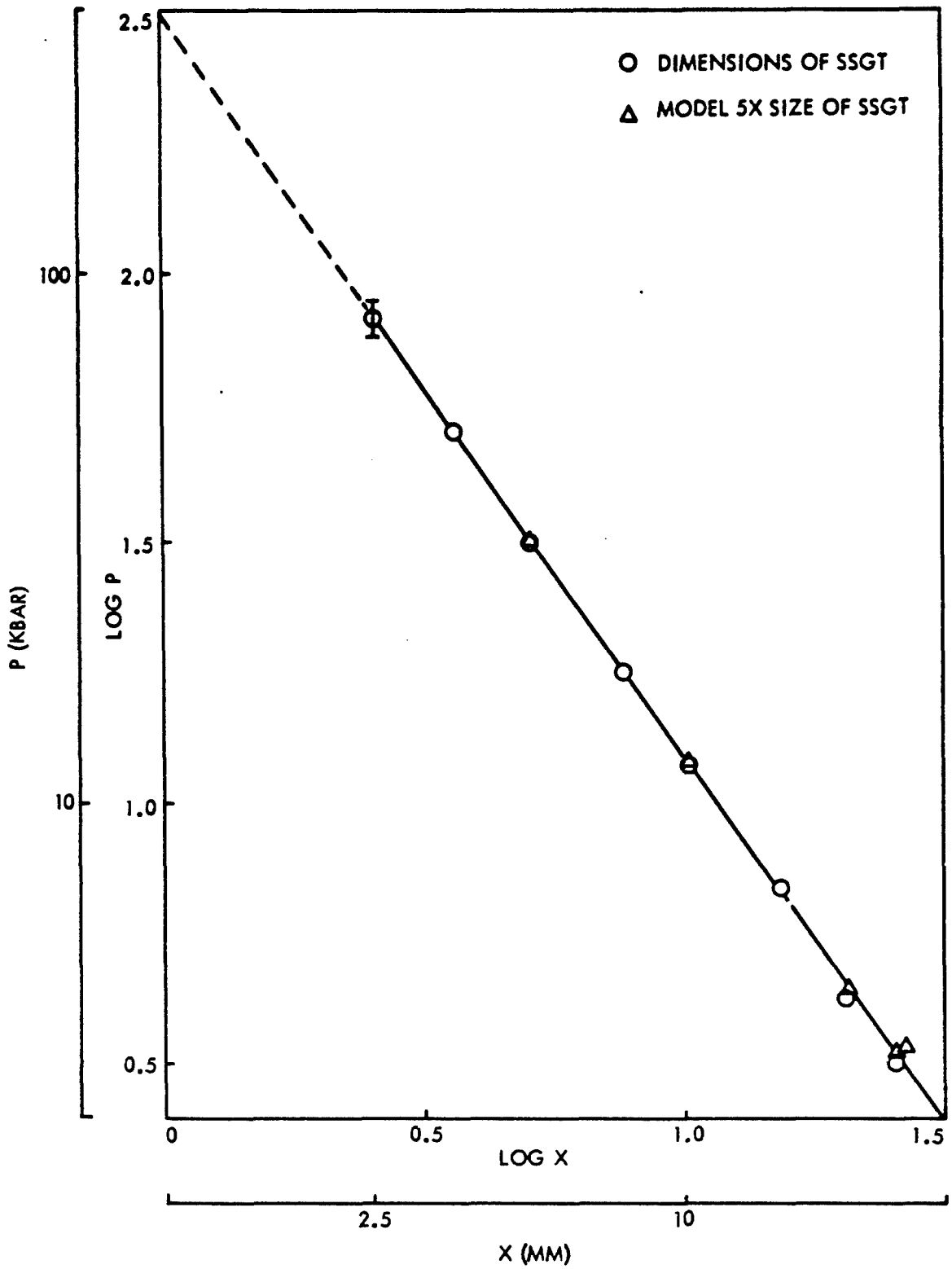


FIG. 7 CALIBRATION DATA FOR SSGT

which makes it quite obvious that the linear extrapolation must fail at X < 2.5 mm, i.e., in the region where measurements could not be made. Otherwise, the pressure required at zero gap would be infinite; this is certainly not the case.

To obtain reasonable nominal values of P at X < 2.5 mm, we estimated the strength of the shock entering PMMA as a result of the detonation of RDX ($\rho_0$ = 1.58 g/cc) adjacent to the PMMA. The intersection of the two P vs u curves: the RDX adiabat[3] and the PMMA Hugoniot[4] gave a value of 216 kbar for the shock at X = 0. With this initial value, we can replot the data of Table 1 in the form log P vs X as in Fig. 8. From this curve we can read nominal values of P at X < 2.5 mm. Moreover, comparison of the curve going smoothly to 216 kbar at X = 0 with that obtained by linear extrapolation of Eqn. (3) indicates that the latter extrapolation is probably adequate down to X = 2 mm (P ~ 115 kbar). The final calibration data for the SSGT are therefore those given in Table 2.

It is of interest to compare the calibration curve for the SSGT with that for the LSGT. For this purpose, we would like better nominal values of P at X = 0 and X = 5 mm than those obtained analytically in Ref. 2. The diagram of the LSGT is shown in Fig. A1; its standard donor is tetryl at $\rho_0$ = 1.51 g/cc. Extrapolation of Ruby Code computations[5] give C-J values of 195 kbar and 1.84 mm/μsec for pressure and particle velocity of this tetryl. By an approximation similar to that used for RDX above, this leads to a value of 155 kbar for the initial pressure in the PMMA. We can now draw the calibration curve for the LSGT (Fig. 9) for comparison with Fig. 8.

In Figs. 8 and 9 the gap thickness has been shown both in millimeters and in donor diameters (d). The LSGT has an unconfined donor (See Fig. A1) whereas the SSGT has a highly confined one. In the LSGT, the gap pressure shows an approximately exponential decay with thickness down to X = 0.5 d. (The curve of Fig. 9 is slightly concave upward rather than linear). At that point the rate of attenuation increases slightly and at 0.7 d it increases markedly. At (X/d) ≥ 0.5, the LSGT also shows approximate linearity in log P vs log X although the P vs X relation is probably affected by rarefactions that may be avoided in the SSGT because of the high confinement. Unfortunately at (X/d) < 0.5, where no lateral rarefaction affects the LSGT results, we cannot compare the two calibrations because measurements cannot be made in this region for the SSGT configuration.

## Arbitrary Units

For the last five years the SSGT results have been reported in arbitrary units, defined as

Best Available Copy



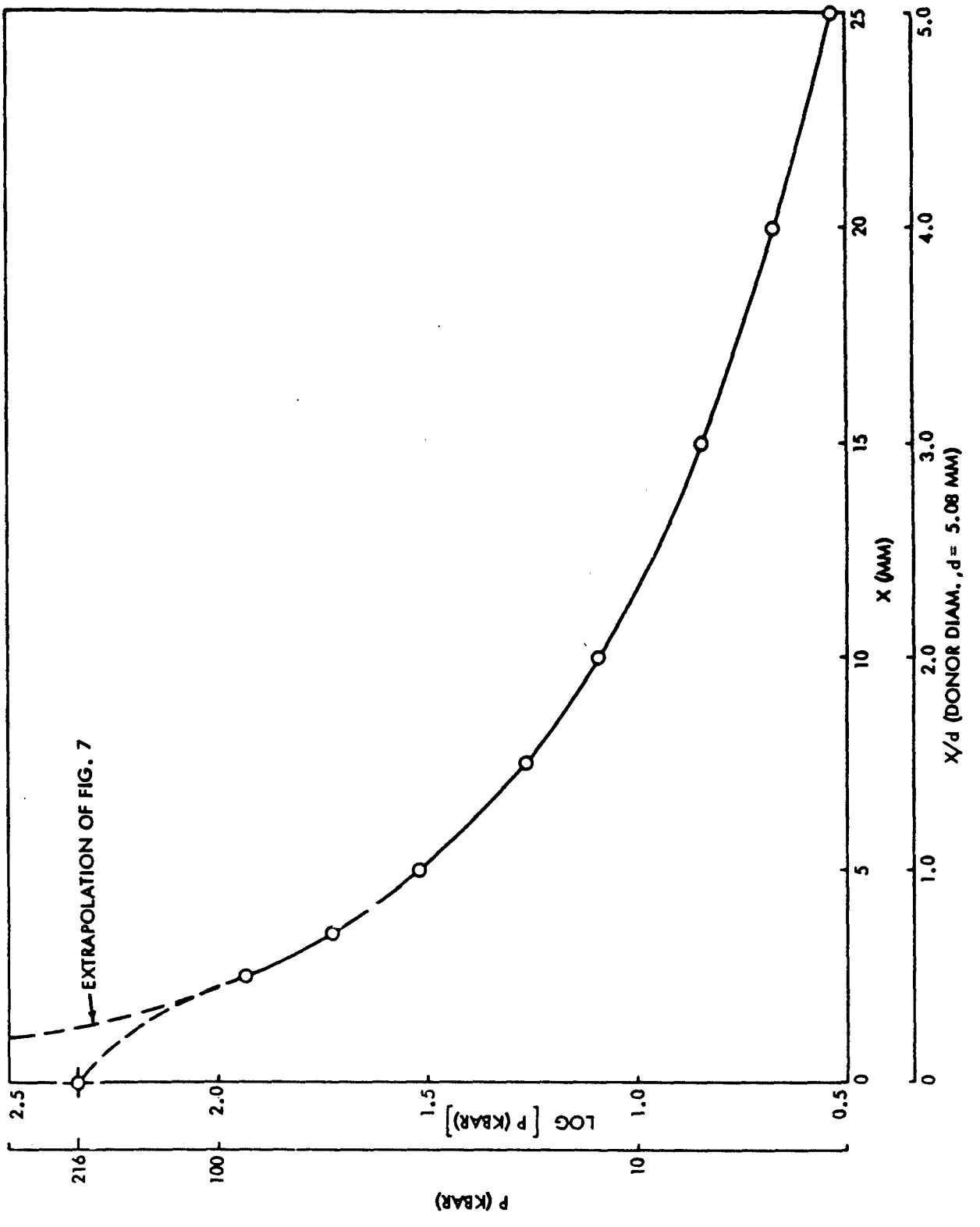


FIG. 8 EXTRAPOLATION OF SSGT CALIBRATION DATA TO ZERO GAP

Best Available Copy

TABLE 2

Calibration Data for SSGT

| X(mm) | P*(kbar) |
|---|---|
| 0 | (216)[a] |
| 2.5 | 85.7 |
| 3.5 | 53.5 |
| 5.0 | 32.5 |
| 7.5 | 18.4 |
| 10.0 | 12.3 |
| 15.0 | 6.7 |
| 20.0 | (4.7)[b] |
| 25.0 | (3.4)[b] |

* From Eqn. (3) of text for X ≥ 2mm

a Nominal value computed as described in text

b Obtained by extrapolation of Fig. 6

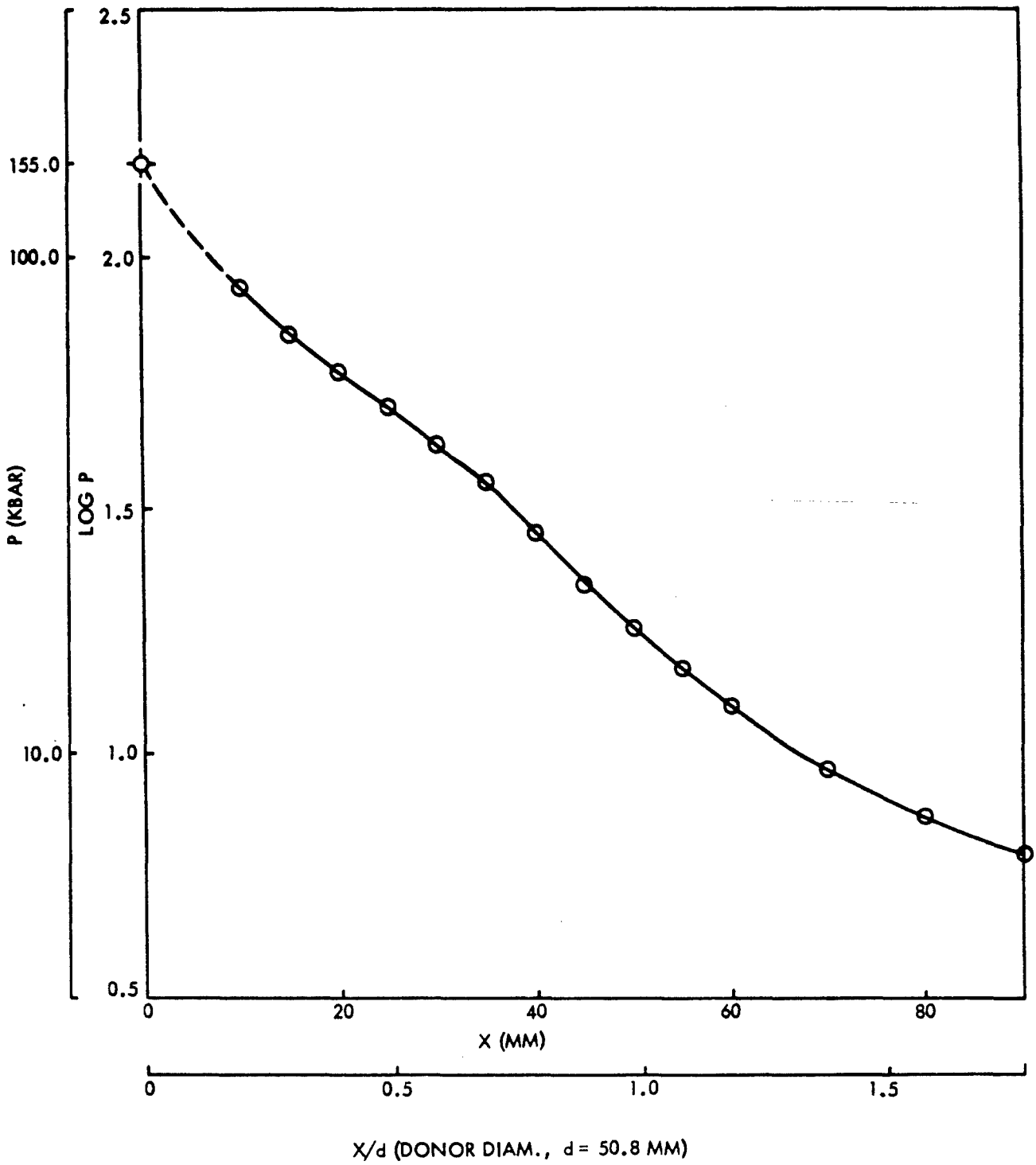


FIG. 9 EXTRAPOLATION OF LSGT CALIBRATION DATA TO ZERO GAP

$$y = A + 10\ B \log \frac{GR}{X} \qquad (5)$$

where A,B = arbitrary constants

GR = reference gap

X = observed 50% gap

and y is in arbitrary units called decibangs. Most commonly the gap is measured in mils. For this unit Eqn (5) becomes

$$y = 30 - 10 \log X \text{ (mils)} \qquad (6)$$

The choice of Eqns (5) and (6) was based on the assumption that the initiating intensity is proportional to the logarithm of the reciprocal gap. If we consider the shock pressure the initiating intensity, Eqn (3) says that this is a good assumption for most values of X. But y(dbg) is not directly proportional to P. Eqns (3) and (6) give

$$\log P = 0.14\ y \text{ (dbg)} + 0.5232 \qquad (7)$$

or

$$P = 3.34 \text{ antilog } (0.14\ y) \qquad (7a)$$

It is therefore incumbent on us to report results henceforth as measured gap thicknesses and the corresponding shock pressures.

When the arbitrary units were used, it was believed that the range of 5 to 17 dbg was adequately covered by the test. We have shown that Eqn (3) may be used up to a pressure of about 115 kbar (ca. 11 dbg); at higher shock strengths, nominal pressures can be obtained from Fig. 8. The lower limit on Eqn (3) is that set by the calibration curve Fig. 6; the curve ends at 5 kbar (less than 2 dbg).

For the reader's convenience, a figure showing the conversion of earlier SSGT results in arbitrary units to $P_g$ (kbar) has been prepared from Eqn (7a). It is Fig. A2 of the first appendix.

## COMPARISON OF TEST VALUES OF SSGT WITH THOSE OF LSGT

To obtain a comparison of the large and small scale tests, six explosives were tested over approximately the same range of % TMD in each case. The same batches of H.E. were used throughout. In addition, earlier data were scanned for explosive batches which had been tested in both configurations.

Best Available Copy



Most of the LSGT data have been previously reported[5]; they are given in Table A2 and six series are plotted in Fig. 10. About half the SSGT data have been reported earlier[8]; data used in this work are given in Table A3 and five series (corresponding to those of Fig. 10) are plotted in Fig. 11. The differences in the apparent shock sensitivities measured by the large and small scale tests will be discussed before the similarities are pointed out.

Subcritical Behavior of NQ

The most obvious difference between Figs. 10 and 11 is the lack of a curve for high bulk density (HBD) nitroguanidine (NQ) in the latter figure. This results, not from sensitivity [As Fig. 10 shows, low bulk density NQ is less sensitive than NQ (HBD).], but from a critical diameter effect. NQ(LBD) consists of hollow needle crystals of about 5μ diam x 60-65 μ long whereas NQ(HBD) consists of irregular but roughly spherical particles of 60-65 μ diam. Consequently the NQ(LBD) has the smaller particle size and hence the smaller critical diameter.

The fact that NQ(HBD) does not detonate in the SSGT can be shown by measuring the output of its charges as a result of shocking them with the firing of the standard donor. Table 3 contains the results of such measurements and they are compared with analogous ones for NQ(LBD) and tetryl (X102) in Fig. 12. This figure shows that NQ(LBD) exhibits an output per density unit equivalent to that of tetryl, which we know detonates. In contrast to this behavior, NQ(HBD) is not producing the output to be expected from its detonation, although it approaches the detonation level as its loading density is lowered. At 56% TMD (1 g/cc) it appears to be just under its critical diameter in the SSGT configuration. Probe measurements confirmed detonation of NQ(LBD) and a fading reaction of NQ(HBD). (See Table A4).

Obviously it is impossible to measure shock sensitivity to detonation if the acceptor cannot detonate, i.e., if the SSGT conditions are subcritical for the test material. Hence no curve for NQ(HBD) appears in Fig. 11. If, however, output and detonation velocity measurements are ignored, and the test is run only on the arbitrary criterion for a positive result, arbitrary test values can, of course, be obtained. A few of these are listed as pseudo 50% values at the bottom of Table 3. They provide an illustration useful in later discussion.

Before leaving the NQ data, it is of interest to point out that the output/$\rho_0$ vs % TMD of this H.E. shows that it belongs to the group of explosives which exhibit a critical diameter increasing with increasing loading density.

Best Available Copy



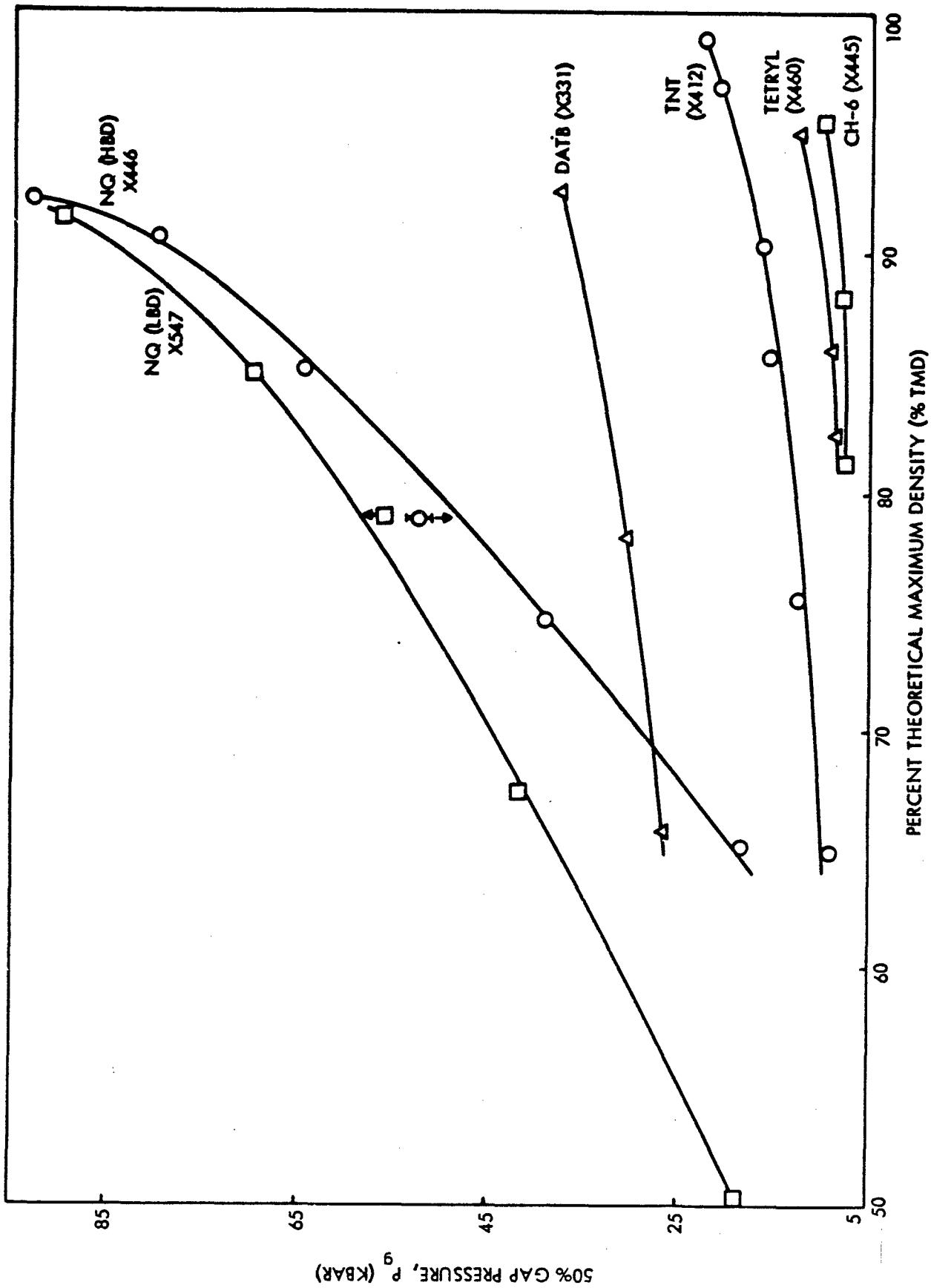


FIG. 10 SHOCK SENSITIVITY AS A FUNCTION OF LOADING DENSITY, LSGT

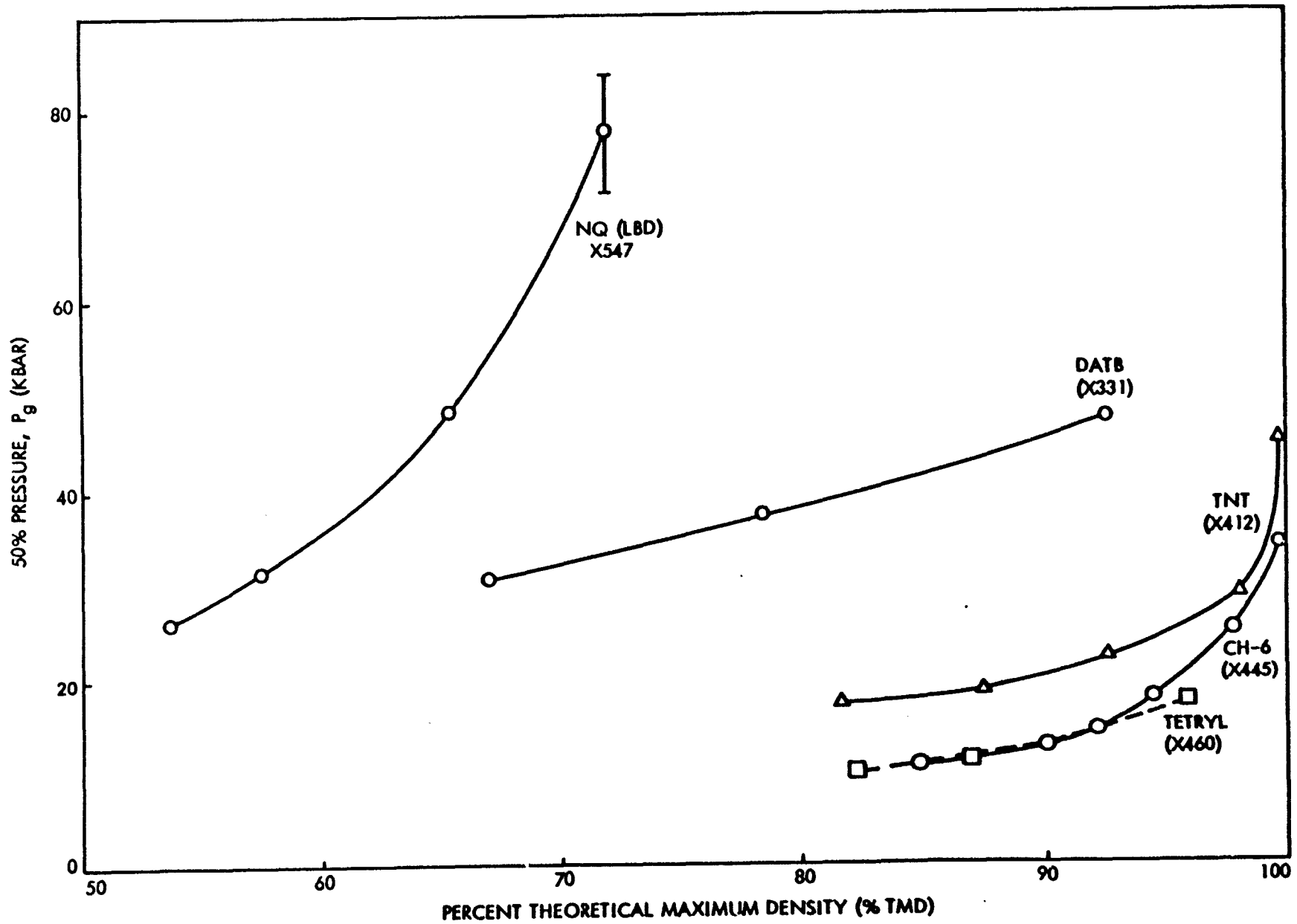


FIG. 11 SHOCK SENSITIVITY AS A FUNCTION OF LOADING DENSITY, SSGT

TABLE 3

Zero Gap Output for High Bulk Density Nitroguanidine (X446)

| Pressure k psi | $\rho_o$ g/cc | % TMD | Output mils | Output/$\rho_o$ |
|---|---|---|---|---|
| 0.25 | 1.0[a] | 56.2 | 25.5[a] | 25.5 |
| 1.0 | 1.16 | 65.1 | 22.7[b] | 19.6 |
| 2.0 | 1.25 | 70.2 | 18.3,16.4 | 13.9 |
| 3.0 | 1.30 | 73.0 | 13.2,17.7 | 11.8 |
| 3.6 | 1.32 | 74.1 | 14.0,12.0 | 9.8 |
| 6.75 | 1.41 | 79.1 | 7.0 2.0 | 3.2 |
| 8.4 | 1.46 | 82.0 | 0.5 0.3 | 0.3 |
| 13.0 | 1.52 | 85.3 | 2.0 2.5 | 1.5 |

a - Six shots with ranges of 0.96 to 1.04 in $\rho_o$ and 23.3 to 30.5 mils in output.

b - Three shots with range of 21.9 to 23.4 mils in output.

Pseudo - 50% Point Values

| Pressure k psi | $\rho_o$ g/cc | % TMD | Arbitrary Units, dbg | $P_g$ kbar |
|---|---|---|---|---|
| 0.25 | 0.95 | 53.3 | 5.6 | 20.3 |
| 1.0 | 1.16 | 65.1 | 9.5 | 71.3 |
| 2.0 | 1.25 | 70.2 | 12.0* | 140* |

* X = 1.6 mm, P ≅ 140 from Fig. 8.

Best Available Copy

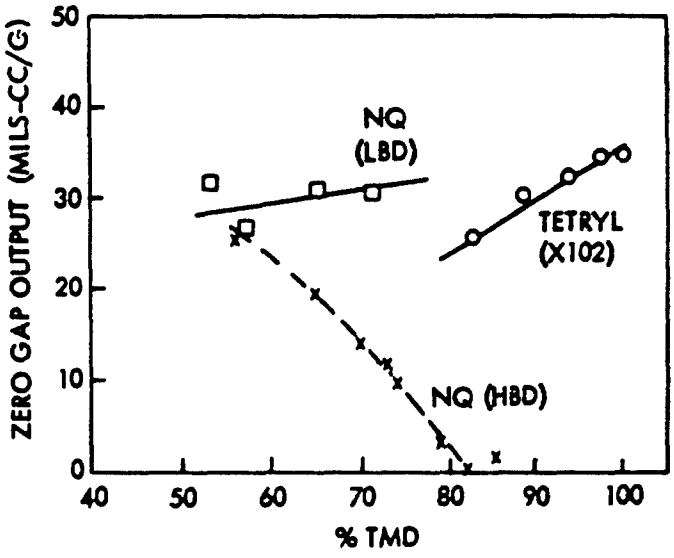


FIG. 12 OUTPUT (DENT/$\rho_o$) AT ZERO GAP FOR TWO NITROGUANIDINES AND TETRYL, SSGT

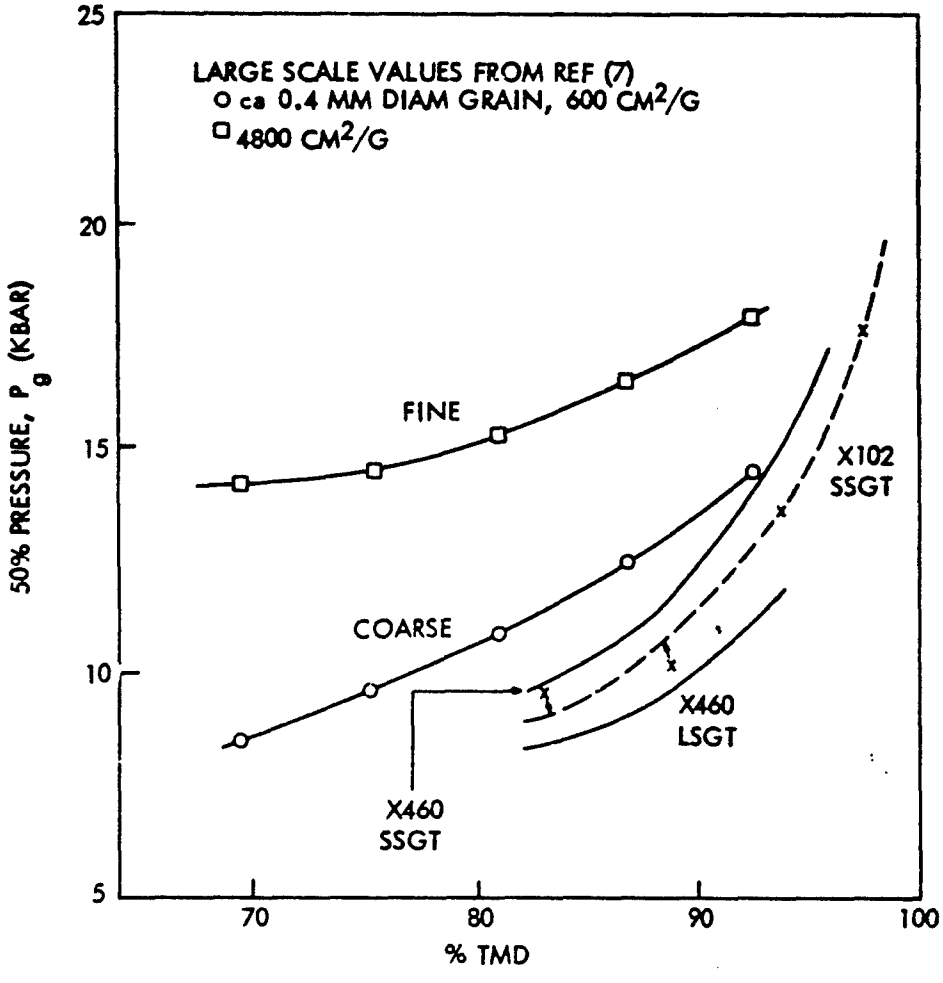


FIG. 13 EFFECT OF PARTICLE SIZE ON SHOCK SENSITIVITY OF TETRYL

Best Available Copy

Particle Size Effect on Measured Sensitivity

A second difference between Figs. 10 and 11 is a sharp decrease in sensitivity indicated by the SSGT values above 95% TMD for TNT and somewhat earlier for CH-6; no correspondingly sharp change in slope occurs in the curves of the LSGT results. Although the SSGT results for DATB (X331) and tetryl (X460) do not appear to show such a sharp change in Fig. 11, DATB (X315) and tetryl (X102), which were pressed to higher % TMD, did show it (See Table A3). We believe that this difference will appear whenever the large charges can be pressed to as high % TMD as the small, and that it is chiefly a particle size effect.

It now seems established that in many cases of granular charges at atmospheric pressure, coarser materials are more shock sensitive than fine. Seely[7] has shown this for tetryl and PETN over a range in % TMD; Chick[8] has shown it for HMX ($\rho_0$ = 1 g/cc); and our results show it for NQ. Seely's results for fine and coarse tetryl are given as 50% gap vs $\rho_0$[7]. However, they were carried out on the large scale LASL test which is partially described in Ref. 9. It is a 1-5/8-in. diam test, acceptor unconfined, and donor of about 2.5 $\ell$/d. The gap material was PMMA[7] and the 50% gaps for tetryl ranged from 2 to 3 in. Although the donor explosive is not specified, it has been found that tetryl calibration curves for various $\ell$/d converge at about 1.4 diameters of the attenuator and a common curve can be used at the greater gap thicknesses[10]. Moreover, pentolite and tetryl boosters give a common calibration at these high attenuations[2]. In view of this situation which suggests equivalence of the highly attenuated shock from different donors, the NOL data for calibration of the LSGT (Table A1), which is 2-in. diam for the donor/gap system, should give a rough approximation to the calibration of the 1-5/8-in. diam test.

The tetryl data of Ref. 7 have been converted to $P_g$ vs % TMD by using the above approximation. They are displayed on a very much magnified pressure scale in Fig. 13. Also shown for comparison are the NOL results: LSGT and SSGT (on two different lots of tetryl). The LSGT results parallel those of Ref. 7 and show the proper sign of the sensitivity difference to be expected as a result of confinement. Thus at 90% TMD, $P_g$ for coarse unconfined tetryl is 13.6 kbar; that for the LSGT on lot X460 is 10.1 kbar. (This is a larger effect than would be expected at this sensitivity level. The difference is 1-2 kbar for pentolite[5]. However, the exact position of the Ref. 7 curves is not important to the illustration.)

The SSGT curves for tetryl lots X460 and X102 are both shown because the latter covers the range up to 100% TMD and parallels the former for which the LSGT data are also available.

The SSGT curves lie above the LSGT data, as would be expected from an acceptor diam effect on $P_g$. But the more important point here is that although the large scale curves[7] show that the coarse tetryl is more shock sensitive than the fine, the two curves are gradually approaching each other as the % TMD increases. Both this approach and the steep rise of the SSGT curves can very reasonably be attributed to fracture of the coarser particles as the charge is compressed under higher and higher pressures. This is a process that will occur most readily in coarse materials and under the conditions of hydraulic pressing used in the SSGT. If it occurs, it means that the particle size of the initially coarse material varies along the entire curve until, at high densities, the charge's average particle size, as well as its sensitivity, are those of the initially finer material.

If crushing of the explosive particles is the dominant cause of the sharp decrease in sensitivity at high % TMD in the SSGT results, this decrease should appear less and less as the initial particle size of the material decreases. The suggested mechanism can be further investigated by running SSGT determinations on superfine explosive to as high % TMD as can be achieved.

Apparent Reversals in Sensitivity Ratings

Seely also showed an apparent reversal in the sensitivity of his fine and coarse tetryls with the test scale used[7]. Fig. 14 reproduces his results. At very high $\rho_o$, the small scale test results on the two tetryl samples are the same. This would be expected from the particle size effect discussed above. But for $\rho_o < 1.6$ g/cc, the results in the smaller test (Fig. 14b) are the reverse of those in the large (Fig. 14a), i.e., the coarse tetryl appears less sensitive than the fine when tested on the smaller scale. Tetryl is a material for which the critical diameter increases with decreasing $\rho_o$. Moreover, all explosives exhibit increasing critical diameter with increasing particle size. Hence it is suggested that the smaller scale test is subcritical for coarse tetryl at $\rho_o < 1.6$ g/cc, and that the apparent reversal stems from failure to detonate the coarse tetryl in this test. (Seely pointed out that in the region $\rho_o < 1.3$ g/cc, he had to increase the acceptor length to obtain sharp results from measured plate dents.*)

*In a recent conversation, Seely said that he believed he had obtained detonation of the coarse tetryl in his small scale test. For a few tests at low $\rho_o$, he had used a granular bed, at the same $\rho_o$, following the small scale test column, and had placed foil switches in the granular bed. Detonation did occur in the granular bed. Without further details, it still seems possible that detonation was not achieved in the half-inch diameter column although vigorous reaction undoubtedly did occur.

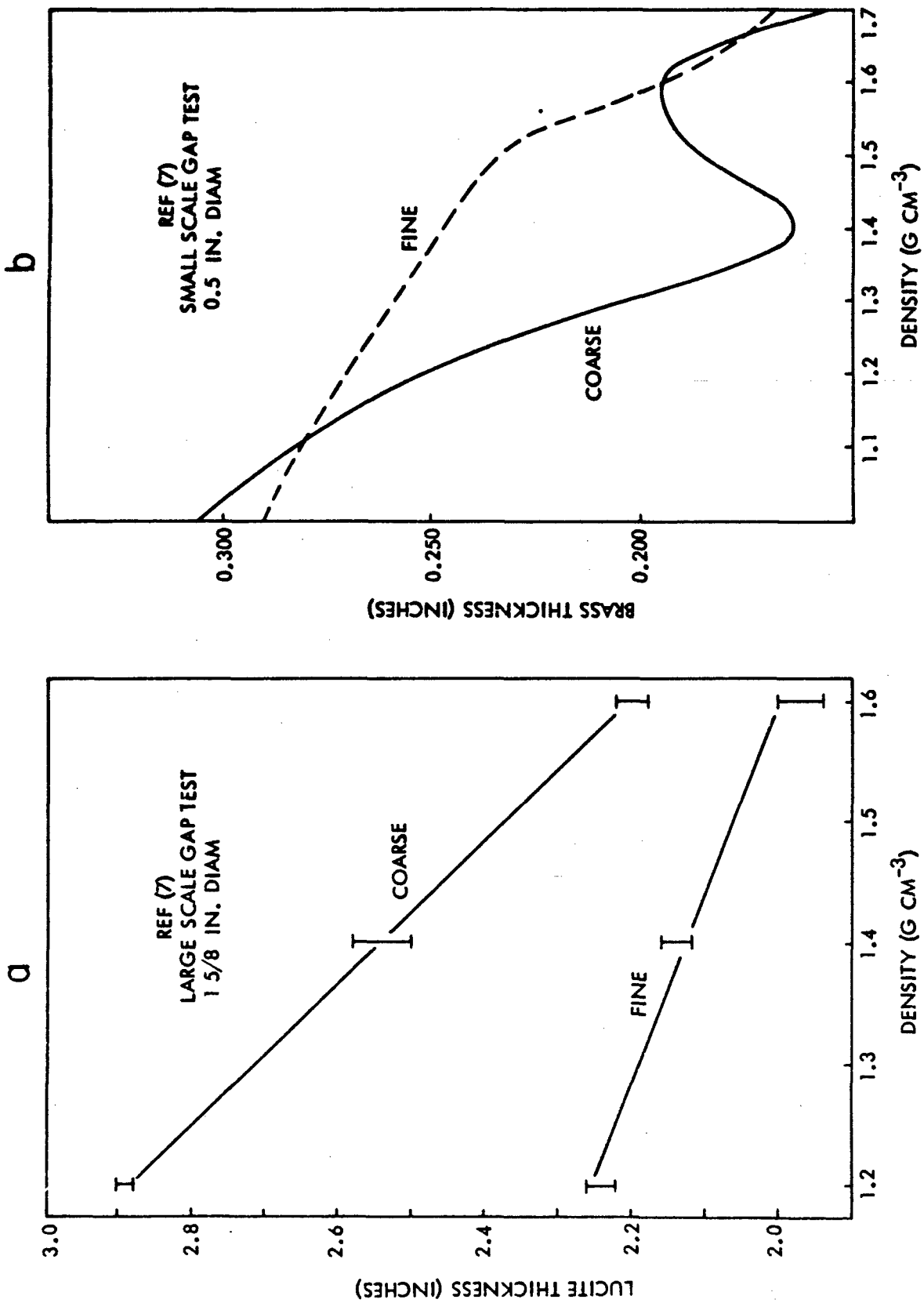


FIG. 14 APPARENT REVERSAL OF TETRYL SENSITIVITY WITH CHANGE IN TEST FROM LARGE TO SMALL SCALE

We can show a false reversal in the present data. In this case, we know that subcritical conditions are responsible for the fictitious reversal as we believe they are in the case above. Figure 10 shows the LSGT result that NQ(LBD) is less sensitive than NQ(HBD) at TMD ≤ 90%. Figure 15 compares the NQ(LBD) curve from the SSGT results with the pseudo 50% values given at the bottom of Table 3. These latter were obtained, as described earlier, by using the arbitrary criterion of a positive test result despite the fact that the acceptor did not reach detonation. As Fig. 15 shows, the pseudo curve for NQ(HBD) lies above the curve for NQ(LBD) and thereby suggests reversal of ratings.

Since we have said repeatedly that the coarse material is more shock sensitive than the fine, it is well to emphasize that this is true only for granular charges at 1 atm and lower pressures. Seely has shown that when the air (or other gas) is replaced by water, a condensed medium, the material of greater surface area (finer particle size) exhibits the higher shock sensitivity. Presumably this will be the case also with other voidless formulations, e.g., H.E. particles embedded in an organic matrix. Moreover, it must mean that the mechanism of shock initiation differs in the two cases.

A third difference between Figs. 10 and 11 is the behavior of CH-6 in the SSGT. CH-6 exhibits its sharp decrease in sensitivity at about 90% TMD rather than the 94 or 95% TMD shown by the other materials in Fig. 11. As a result, the apparent sensitivities of tetryl and CH-6 are reversed by the SSGT values above 90% TMD. This is easier to see in Fig. 16 where the CH-6 curve is compared to a number of other explosives on a magnified pressure scale.

CH-6 is 97.5% RDX, 1.5% calcium stearate, 0.5% graphite, and 0.5% polyisobutylene; in other words it contains 2.5% lubricant. EPM-2 is the HMX analog. Conceivably, in addition to particle crushing, such a material might undergo a homogenization when highly pressed in the SSGT configuration. The small scale charges are prepared by hydrostatic incremental pressing in the 5-mm bore of a heavy brass container; the larger charges are prepared by isostatic pressing and subsequent machining to a final diameter of 36.6 mm. It might well be that more physically homogeneous charges were obtained in the small scale preparations of mixtures of H.E. and a lubricant; if homogenization does occur, it would be expected to reduce the shock sensitivity of the material. As Fig. 16 shows, RDX alone, the HMX analog of CH-6, tetryl, and TNT all show parallel $P_g$ vs % TMD curves up to 94 or 95% TMD. Only CH-6 of these five materials exhibits the rise starting at 90% TMD and consequently shows a reversal in the ratings of tetryl and CH-6, and of

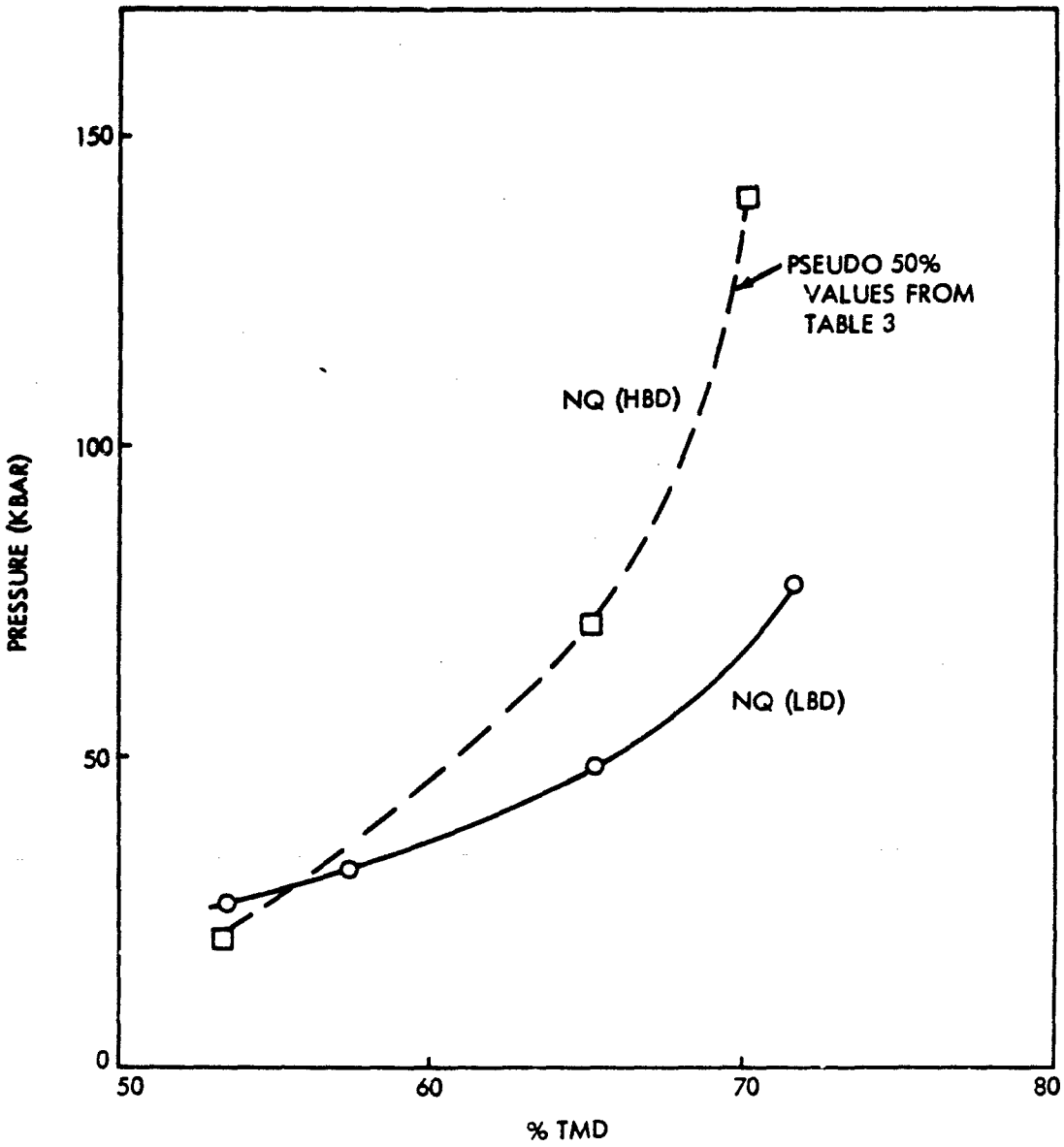


FIG. 15 EXAMPLE OF FICTITIOUS SENSITIVITY REVERSAL USING SSGT RESULTS

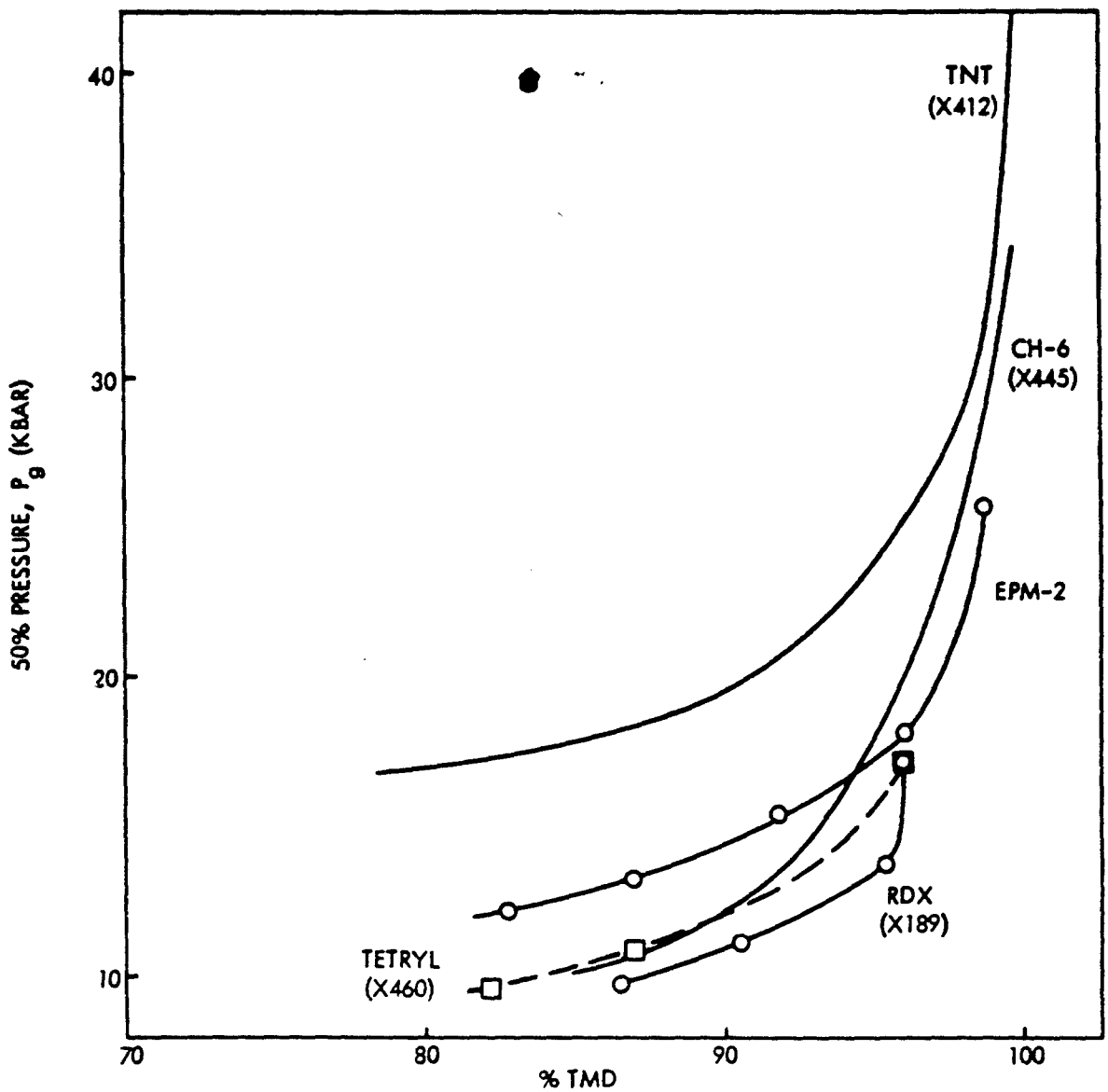


FIG. 16 COMPARISON OF SSGT RESULTS FOR SEVERAL EXPLOSIVES

EPM-2 and CH-6 for TMD values above and below 90%.

Six other lots of CH-6 have been run on the SSGT. Of these, half paralleled the RDX curve up to 93% TMD; the rest, up to 92%. It is evident that generally CH-6 will show its sharp decrease in sensitivity at a lower % TMD than the other materials studied.

To summarize our information so far, we know that correlation between the SSGT and LSGT results requires:

(a) The material must be supercritical in both tests. Generally, this means it must be supercritical in the SSGT.

(b) It must be tested at a TMD of 90% or less in the SSGT to avoid the effect on $P_g$ tentatively attributed to particle crushing and possibly to charge homogenization as well. (If no material such as CH-6 is included, the upper limit can be raised to 94% TMD.)

Table 4 contains the SSGT and LSGT results at the same % TMD, and a number are plotted in Fig. 17 to illustrate point (b) above. The CH-6 data depart from the general trend at 90% TMD; the TNT at 94%. Also included is the single point for Comp C-3, an RDX composition containing 22% plasticizer. Although the % TMD of this charge is unknown it is evidently high, judged by its large departure from the general trend.

## Correlation between the Small and Large Scale Test Results

The differences between Figs. 10 and 11 have been explored so that comparison of the LSGT and SSGT data can be made on a sound basis. The general likenesses are $P_g$ vs % TMD curves that are concave upward and a qualitative sensitivity rating of the same order at the lower % TMD. The most important practical result is that the SSGT values will not correlate with the LSGT values from explosive to explosive if the test are carried out at high % TMD (above 94% for most H.E., above 90% TMD for waxed or plasticized explosives). All the data of Table 4 except those in this low porosity region are plotted in Fig. 18. With care in selecting the % TMD for testing, an excellent quantitative correlation is found between the results of the two tests.

It is well known that there is a dependence of the measured $P_g$ on the effective diameter of the charge. Near the detonability limits, a pressure near the detonation pressure of the acceptor might be required. But as the conditions become supercritical, the explosive becomes easier to initiate. In particular, as the effective diameter increases the required $P_g$ decreases for heterogeneous H.E., and asymptotically approaches

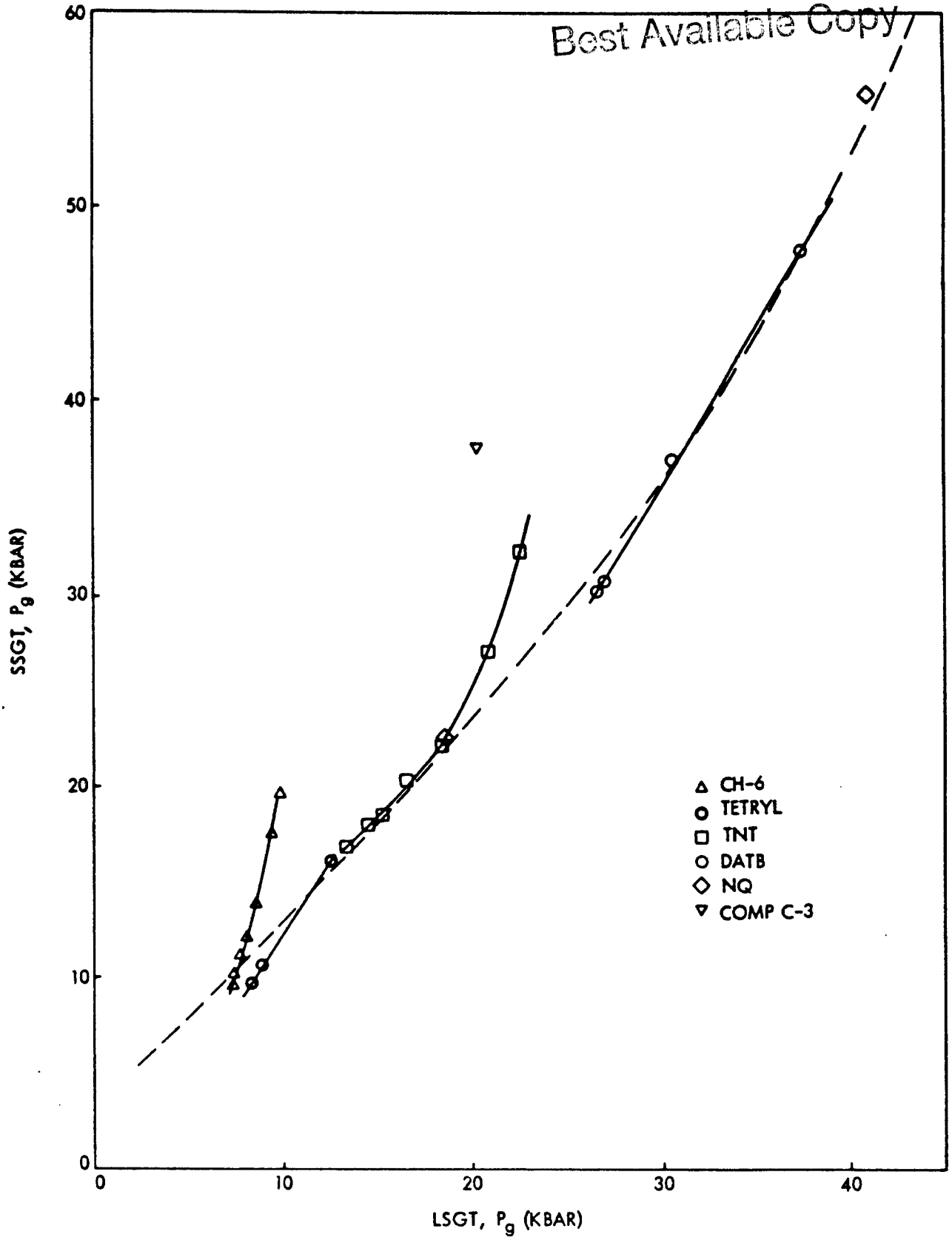


FIG. 17 COMPARISON OF DATA FROM LSGT WITH THOSE FROM SSGT UP TO 60 KBAR IN LATTER

TABLE 4

COMPARISON OF LSGT AND SSGT RESULTS AT SAME % TMD

| Material | $\rho_o$ | % TMD | 50% Pressure $P_g$ (kbar) LSGT | SSGT |
|---|---|---|---|---|
| NQ (LBD) X547 | 0.56 | 31.2 | [15.2] | - |
| | 0.90 | 50.3 | 18.5 | 22.5** |
| | 1.20 | 67.4 | 41.0 | 55.7* |
| | 1.27 | 71.5 | 46.8* | 77.5 |
| DATB X331 | 1.21 | 65.8 | 26.5 | 30.2** |
| | 1.23 | 67.0 | 26.9* | 30.7 |
| | 1.44 | 78.1 | 30.5 | 37.0* |
| | 1.70 | 92.5 | 37.5 | 47.4 |
| TNT X412 | 1.35 | 81.8 | 13.2* | 17.1 |
| | 1.42 | 85.7 | 14.5 | 18.0* |
| | 1.45 | 87.4 | 15.2* | 18.5 |
| | 1.49 | 90.3 | 16.5 | 20.3* |
| | 1.55 | 93.6 | 18.4* | 22.2 |
| | 1.60 | 96.9 | 20.8 | 27.0* |
| | 1.64 | 98.9 | 22.6 | 32.5* |
| TATB | 1.82 | 93.9 | 58.8 | (101.7)*** |

| Material | $\rho_o$ | % TMD | 50% Pressure $P_g$ (kbar) LSGT | SSGT |
|---|---|---|---|---|
| Tetryl X412 | 1.43 | 82.4 | 8.3 | 9.7* |
| | 1.49 | 86.0 | 8.9 | 10.6* |
| | 1.64 | 94.9 | 12.5 | 16.1* |
| CH-6 X445 | 1.45 | 81.3 | 7.3 | 9.6** |
| | 1.51 | 84.9 | 7.4* | 10.2 |
| | 1.57 | 88.2 | 7.7 | 11.2* |
| | 1.60 | 90.0 | 8.1* | 12.1 |
| | 1.64 | 92.1 | 8.6* | 14.0 |
| | 1.68 | 94.4 | 9.4* | 17.6 |
| | 1.70 | 95.5 | 9.9 | 19.7* |
| RDX X189 | 1.53 | 85.0 | 6.5 | 9.3** |
| | 1.64 | 91.8 | 7.0 | 11.5* |
| EPM-2 | 1.72 | 91.7 | 13.1 | 15.5 |
| Comp C3 | 1.61 | - | 20.2 | 37.6 |

* Interpolated
** Extrapolated
*** Nominal value from Fig. 8

Best Available Copy

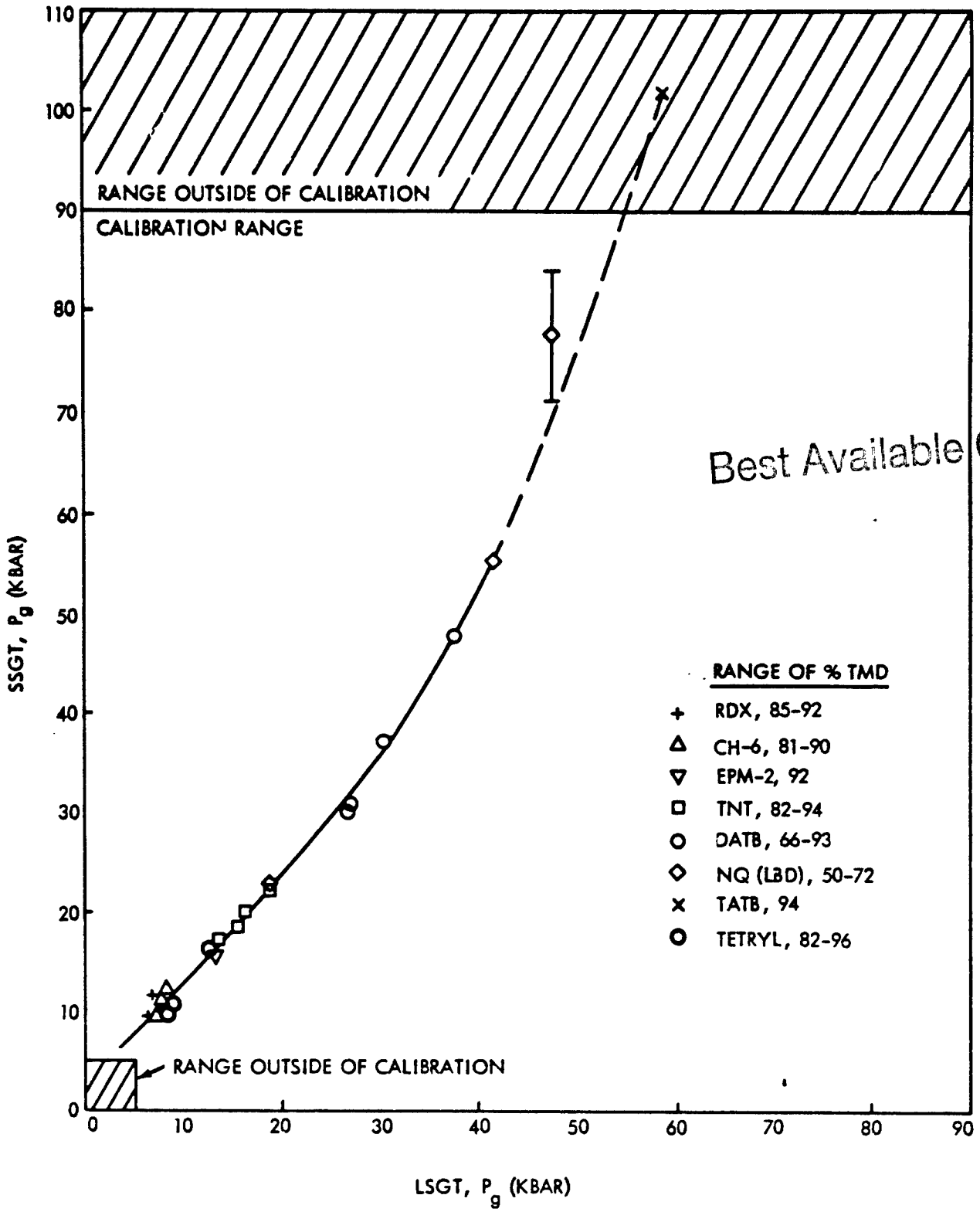


Best Available Copy

FIG. 18 CORRELATION OF SSGT AND LSGT VALUES

its infinite diameter value. Since the effective diameter of the SSGT is certainly smaller than that of the LSGT, $P_g$ measured in the former will be larger than $P_g$ measured in the latter. Moreover, the percentage difference will increase as the sensitivity decreases; this trend is indicated by the confinement effect on LSGT $P_g$ values.[5]

Figure 18 is a plot of SSGT $P_g$ vs LSGT $P_g$ of all data of Table 4 except the values for charges at very high % TMD, as discussed above. The correlation is excellent and shows exactly the trends to be expected on the basis of our present knowledge of the shock-to-detonation behavior of explosives. Additional data for explosives fired in both tests should be collected routinely, and perhaps a special study should be made of a highly waxed explosive which can be prepared at various % TMD. Subsequently the comparison of Fig. 18 should be repeated and the curve either confirmed or modified.

## SUMMARY

The SSGT has been calibrated over the range of 5 to 90 kbar. An analytical relation between thickness of PMMA gap and $P_g$ is given and its use in the range 3-115 kbar justified. A method of determining nominal values of $P_g$ > 115 kbar is also presented.

Comparison of the results obtained in the SSGT with those of the LSGT show an excellent correlation provided the tests are made at % TMD ≤ 90. At higher % TMD (lower porosities) the SSGT values show a very rapid decrease in sensitivity with decreasing porosity; the LSGT values do not exhibit this behavior. Consequently, tests carried out at very low sample porosity can show apparent reversal in rating from explosive to explosive with change from a small to large scale test.

Differences between the two tests at high % TMD have been attributed chiefly to a particle size effect especially evident in the SSGT where crushing of the particles under high pressures might be expected. When the test conditions were chosen to avoid this region, we found no true reversals in sensitivity measured on the large and small scale tests. There was, however, one instance of apparent reversal which resulted from applying an arbitrary criterion to a test material which was subcritical in the SSGT. This was described in detail because it affords a basis for judging reversals reported by other investigators.

## ACKNOWLEDGMENT

Many people have contributed to the work reported here. In particular we wish to thank C. Randall and J. Ayres for SSGT results, G. Roberson and I. Jaffe for LSGT results, and J. Schneider for the surface velocity and shock velocity measurements.

## REFERENCES AND NOTES


1. J. N. Ayres, "Standardization of the Small Scale Gap Test Used to Measure the Sensitivity of Explosives", NavWeps 7342 (16 Jan 1961).

2. T. P. Liddiard, Jr. and D. Price, "Recalibration of the Standard Card-Gap Test", NOLTR 65-43 (20 Aug 1965).

3. Computed for polytropic expansion with $\gamma = 2.736$. This value was derived from data for RDX ($\rho_0 = 1.59$) in Chem. Revs. 59, 801 (1959).

4. Coleburn's Hugoniot for PMMA,

$$U = 2.710 + 1.568u - 0.037u^2$$

was used because it as well as the adiabat above were easily available in working curves set up by H. M. Sternberg and W. A. Walker. In the high pressure region this relation and that of Table A1 give essentially the same results.

5. I. Jaffe, G. E. Roberson, A. R. Clairmont, Jr., and D. Price, "The NOL Large Scale Gap Test. Compilation of Data for Propellants and Explosives II", NOLTR 65-177, 15 Nov 1965. Confidential.

6. J. N. Ayres, "Explosive Properties from Small Scale Gap Test Measurements", Discussion at E.R.D.E., Waltham Abbey, 4 Oct 1963. Confidential.

7. L. B. Seely, "A Proposed Mechanism for Shock Initiation of Low Density Granular Explosives", Proceedings of Fourth Electric Initiator Symposium at Franklin Institute, Phila. 1963. Paper 27 of Rept EIS-A2357.

8. M. C. Chick, "Effect of Interstitial Gas on the Shock Sensitivity of Low Density Explosive Compacts", Paper C-132 in preprints of Fourth Detonation Symposium (1965).

9. A. Popolato, "Experimental Techniques Used at LASL to Evaluate Sensitivity of High Explosives", Proceedings of the International Conference on Sensitivity and Hazards of Explosives, London, Oct. 1963.

10. I. Jaffe and A. R. Clairmont, "The Effect of Configuration and Confinement on Booster Characteristics", NOLTR 65-33 (13 Apr 1965).

11. J. N. Ayres, L. D. Hampton, I. Kabik, and A. D. Solem, "Varicomp. A Method for Determining Detonation-Transfer Probabilities". NavWeps 7411 (30 June 1961).

Best Available Copy

# APPENDIX A

Best Available Copy

## Supplementary Data

This appendix supplies data supplementary to that in the text. Table A1 contains the calibration data for the LSGT; they are repeated from Ref. (2) to make the present report more convenient. Similarly, Fig. A1 is a diagram of the LSGT. Charges for the first six series of Table A1 were very carefully prepared. Consequently, the precision of the 50% gap should be better than ±0.2 mm (except where a range is given) and that of the loading density, ±0.01 g/cc (except for the handpacked charges).

Table A3 contains the detailed SSGT data used in the report; statistical variations are indicated in the table. In Table A4 are recorded the individual results of a few probe measurements made on NQ in the SSGT configuration. They confirm the conclusions from the observed zero gap output, that the NQ (LBD) is detonating in the SSGT and that the NQ (HBD) is not. It is interesting, however, that the standard donor initiates a reaction in the latter that has not completely faded after a failing propagation of 7.5 charge diameters; in this high confinement, the effective charge diameter is not known.

Fig. A2 can be used for rapid, approximate conversion of earlier SSGT results in arbitrary units to $P_g$(kbar) from the present calibration.

TABLE A1

HUGONIOT DATA FOR PMMA AND CALIBRATION DATA FOR LSGT*

| Gap Length X(mm) | $P_g$ kbar | U mm/μsec | u mm/μsec |
|---|---|---|---|
| 0 | (126.0) | (5.75) | (1.86)** |
| 5 | (104.7) | (5.27) | (1.68) |
| 10 | 86.2 | 4.94 | 1.48 |
| 15 | 69.9 | 4.63 | 1.28 |
| 20 | 58.7 | 4.39 | 1.13 |
| 25 | 50.0 | 4.19 | 1.01 |
| 30 | 42.4 | 4.01 | 0.896 |
| 35 | 35.7 | 3.84 | 0.788 |
| 40 | 28.1 | 3.66 | 0.651 |
| 45 | 22.0 | 3.50 | 0.533 |
| 50 | 18.0 | 3.40 | 0.449 |
| 55 | 14.9 | 3.34 | 0.378 |
| 60 | 12.4 | 3.28 | 0.320 |
| 70 | 9.2 | 3.20 | 0.244 |
| 80 | 7.4 | 3.15 | 0.199 |
| 90 | 6.2 | 3.12 | 0.168 |
| 100 | 5.3 | 3.10 | 0.145 |

$U = 2.57 + 1.61\ u$ $\qquad$ $u \geq 0.75$ mm/μsec

* Data from Ref (2)

** Values in parentheses nominal, not measured. Supplementary data from Fig (9) are:

| Gap Length X(mm) | $P_g$ kbar | U mm/μsec | u mm/μsec |
|---|---|---|---|
| 0 | 155 | 6.00 | 2.20 |
| 5 | 111 | - | - |

Best Available Copy

TABLE A2

DATA OBTAINED WITH LSGT

| Material | $\rho_o$ | % TMD | 50% Values Gap No. Card | 50% Values Gap mm | 50% Values $P_g$ kbar |
|---|---|---|---|---|---|
| NQ | 0.56* | 31.2 | 215-216 | 54.6-54.9 | 15.4-15.1 |
| X547 | 0.90 | 50.3 | 194 | 49.3 | 18.5 |
| (LBD) | 1.20 | 67.4 | 121 | 30.7 | 41.5 |
| | 1.41 | 78.9 | 83-85 | 21.1-21.6 | 56.5-55.5 |
| | 1.51 | 85.0 | 60 | 15.2 | 69.5 |
| | 1.63 | 91.4 | 35 | 8.9 | 90.0 |
| NQ | 1.16* | 65.1 | 196 | 49.8 | 18.3 |
| X446 | 1.33 | 74.7 | 128 | 32.5 | 39.0 |
| (HBD) | 1.40 | 78.9 | 90-95 | 22.9-24.1 | 53.2-51.3 |
| | 1.51 | 85.1 | 68 | 17.3 | 64.2 |
| | 1.61 | 90.6 | 47 | 11.9 | 79.7 |
| | 1.64 | 92.1 | 32 | 8.1 | 93.0 |
| DATB | 1.21 | 65.8 | 162 | 41.2 | 26.5 |
| X331 | 1.44 | 78.1 | 151 | 38.4 | 30.5 |
| | 1.70 | 92.5 | 132 | 33.5 | 37.5 |
| TNT | 1.07* | 64.9 | 282 | 71.6 | 8.9 |
| X412 | 1.25** | 75.6 | 239 | 60.7 | 12.3 |
| | 1.42 | 85.7 | 213 | 54.1 | 15.5 |
| | 1.49 | 90.3 | 208 | 52.8 | 16.2 |
| | 1.60 | 96.9 | 183 | 46.5 | 20.8 |
| | 1.64 | 98.9 | 175 | 44.5 | 22.6 |

* Hand packed

** Hydrostatically pressed by increments. All others by isostatic pressing.

TABLE A2 CONT.

DATA OBTAINED WITH LSGT

| Material | $\rho_o$ | % TMD | 50% Values Gap No. Card | 50% Values Gap mm | 50% Values $P_g$ kbar |
|---|---|---|---|---|---|
| Tetryl | 1.43 | 82.4 | 294 | 74.7 | 8.3 |
| X460 | 1.49 | 86.0 | 283 | 71.9 | 8.9 |
| | 1.64 | 94.9 | 238 | 60.4 | 12.5 |
| CH-6[a] | 1.45 | 81.3 | 314 | 79.8 | 7.3 |
| X445 | 1.57 | 88.2 | 306 | 77.7 | 7.7 |
| | 1.70 | 95.5 | 267 | 67.8 | 9.9 |
| RDX | 1.64 | 91.8 | 323 | 82.0 | 7.0 |
| X189 | 1.53 | 85.0 | 336 | 85.3 | 6.5 |
| EPM-2[b] | 1.72 | 91.7 | 232 | 58.9 | 13.1 |
| TATB X406 | 1.82 | 93.9 | 78 | 19.8 | 59.0 |
| Comp C3 | 1.60 | - | 186 | 47.2 | 20.2 |

a. CH-6 is RDX/calcium stearate/graphite/polyisobutylene, 97.5/1.5/0.5/0.5. Its voidless density is taken as 1.78 g/cc, the highest experimental value obtained in SSGT.

b. HMX analog of CH-6. Voidless density is 1.875 g/cc by computation based on 1.78 g/cc for CH-6.

TABLE A3 - Data Obtained with SSGT

| Loading Pressure kpsi | Loading density $\rho_o$ g/cc | % TMD | Output at zero gap mils | 50% Values $\mu^*$ dbg | $g^*$ dbg | P kbar |
|---|---|---|---|---|---|---|
| **NQ X547 (Low Bulk Density)** | | | | | | |
| 1.3 | 0.95 | 53.5 | 34 | 6.39 | 0.05 | 26.2 |
| 2.0 | 1.02 | 57.4 | 28 | 6.95 | 0.10 | 31.4 |
| 4.1 | 1.16 | 65.2 | 31 | 8.29 | 0.14 | 48.3 |
| 8.0 | 1.27 | 71.5 | 31 | 9.5<n<10 | -- | 71.3-83.8 |
| **DATB X331** | | | | | | |
| 4.0 | 1.23 | 67.0 | 33 | 6.89 | 0.09 | 30.7 |
| 12.5 | 1.44 | 78.4 | 44 | 7.48 | 0.03 | 37.1 |
| 37.0 | 1.70 | 92.5 | 55 | 8.24 | 0.11 | 47.4 |
| **TNT X412** | | | | | | |
| 4.0 | 1.35 | 81.8 | 49 | 5.07 | 0.03 | 17.1 |
| 8.0 | 1.45 | 87.4 | 57 | 5.32 | 0.03 | 18.5 |
| 16.0 | 1.55 | 93.6 | 52 | 5.88 | 0.06 | 22.2 |
| 32.0 | 1.62 | 98.1 | 59 | 6.70 | 0.04 | 29.0 |
| 64.0 | 1.65 | 99.8 | 59 | 8.07 | 0.07 | 44.9 |
| **CH-6 X445** | | | | | | |
| 4.0 | 1.51 | 84.9 | 60 | 3.48 | 0.06 | 10.2 |
| 8.0 | 1.60 | 90.0 | 71 | 4.00 | 0.06 | 12.1 |
| 10.0 | 1.64 | 92.1 | 68 | 4.42 | 0.07 | 13.9 |
| 16.0 | 1.68 | 94.4 | 70 | 5.16 | 0.05 | 17.6 |
| 32.0 | 1.74 | 97.8 | 69 | 6.24 | 0.03 | 24.9 |
| 64.0 | 1.77 | 99.7 | 68 | 7.23 | 0.06 | 34.3 |
| **Tetryl X460** | | | | | | |
| 3.0 | 1.42 | 82.2 | 51 | 3.29 | 0.04 | 9.6 |
| 5.3 | 1.50 | 86.9 | 55 | 3.68 | 0.03 | 10.9 |
| 24.0 | 1.66 | 95.9 | 63 | 5.08 | 0.04 | 17.2 |

TABLE A3 - Continued

| Loading Pressure kpsi | Loading density $\rho_o$ g/cc | % TMD | Output at zero gap mils | 50% Values $\mu^*$ dbg | $s^*$ dbg | P kbar |
|---|---|---|---|---|---|---|
| **TATB X406** | | | | | $s^*$ | |
| 4.0 | 1.52 | 78.5 | 43 | 7.92 | 0.04 | 42.9 |
| 8.0 | 1.64 | 85.0 | 46 | 8.56 | 0.14 | 52.7 |
| 16.0 | 1.76 | 91.1 | 50 | 9.63 | 0.10 | 74.4 |
| 32.0 | 1.84 | 95.1 | 51 | 11.10 | 0.10 | (116)[a] |
| 64.0 | 1.89 | 97.6 | 53 | 13.47 | 0.41 | (163)[b] |
| **Tetryl X102** | | | | | | |
| 4.0 | 1.43 | 82.9 | 37 | 3.28 | 0.06 | 9.6 |
| 8.0 | 1.54 | 88.7 | 47 | 3.47 | 0.11 | 10.2 |
| 16.0 | 1.62 | 93.8 | 53 | 4.37 | 0.24 | 13.6 |
| 32.0 | 1.69 | 97.5 | 58 | 5.15 | 0.04 | 17.6 |
| 64.0 | 1.73 | 100.0 | 60 | 6.10 | 0.06 | 23.8 |
| **EPM-2** | | | | | | |
| 4.0 | 1.55 | 82.7 | 46 | 4.02 | 0.05 | 12.2 |
| 8.0 | 1.63 | 86.9 | 58 | 4.28 | 0.17 | 13.3 |
| 16.0 | 1.72 | 91.7 | 57 | 4.77 | 0.06 | 15.5 |
| 32.0 | 1.80 | 96.0 | 65 | 5.27 | 0.06 | 18.2 |
| 64.0 | 1.85 | 98.7 | 65 | 6.33 | 0.05 | 25.7 |
| **RDX (X189)** | | | | | | |
| 10.0 | 1.56 | 86.5 | 50 | 3.28 | 0.05 | 9.8 |
| 18.3 | 1.63 | 90.5 | 53 | 3.77 | 0.08 | 11.2 |
| 31.0 | 1.72 | 95.3 | 60 | 4.41 | 0.15 | 13.8 |
| 38.2 | 1.73 | 96.0 | 59 | 5.07 | 0.36 | 17.1 |





Best Available Copy

TABLE A3 - Concluded

| Loading Pressure kpsi | Loading density $\rho_o$ g/cc | % TMD | Output at zero gap mils | 50% Values $\mu^*$ dbg | $s^*$ dbg | P kbar |
|---|---|---|---|---|---|---|
| Comp C3 | 1.61 | -- | -- | 7.51 | -- | 37.6 |
| DATB (X315) | | | | | | |
| 4 | 1.23 | 67.1 | 36 | 6.94 | 0.04 | 31.2 |
| 10 | 1.46 | 79.2 | 44 | 7.38 | 0.11 | 36.0 |
| 20 | 1.60 | 87.2 | 46 | 7.88 | 0.29 | 42.3 |
| 32 | 1.68 | 91.2 | 52 | 8.10 | 0.04 | 45.4 |
| 64 | 1.76 | 96.0 | 55 | 9.00 | 0.06 | 60.7 |

* The statistical treatment of the sensitivity measurements was performed with the assumption of either a normal or a logistic distribution of the probability of response to the input stimulus, measured in arbitrary units (dbg). The quantity $\mu$ is the stimulus that would cause 50% of the population to respond; it is the same for either distribution provided the distributions are not skewed. The respective population parameters $\sigma$ and $\gamma$ are measures of the broadness of the distribution. For instance, 68% of the normal population will be contained between the limits $\mu \pm \sigma$; 46% of the logistic population, within $\mu \pm \gamma$. Since we can never know the true population values, we use the observed values s and g rather than the true ($\sigma$ and $\gamma$) in the tabulations. See Ref (11) p. 27 et seq. for a detailed discussion of the treatment.

a) Nominal value from Fig. 8 Eqn (3) gives 119 kbar.

b) " " " " " Eqn (3) gives 257 kbar!

Best Available Copy

TABLE A4

IONIZATION PROBE MEASUREMENTS ON NQ IN SSGT CONFIGURATION

| Material | Loading Pressure kpsi | Approx. $\rho_o$ g/cc | Detonation Velocity mm/μsec | | Output mils | |
|---|---|---|---|---|---|---|
| NQ | 1.3 | 0.95 | 4.78, | 4.76 | 25.5, | 26.5 |
| (LBD) | 2.0 | 1.02 | 5.01, | 5.06 | 26.1, | 27.0 |
| X547 | 4.1 | 1.16 | 5.67, | -- | 28.2, | 41.8 |
| | 8.0 | 1.27 | 6.12, | 6.17 | 38.4, | 41.7 |
| NQ (HBD) X446 | 3.6 | 1.32 | Probe 38.1 mm from donor responded; Probe 76.2 mm from donor did not respond. Hence the reaction was fading. | | | |

Best Available Copy

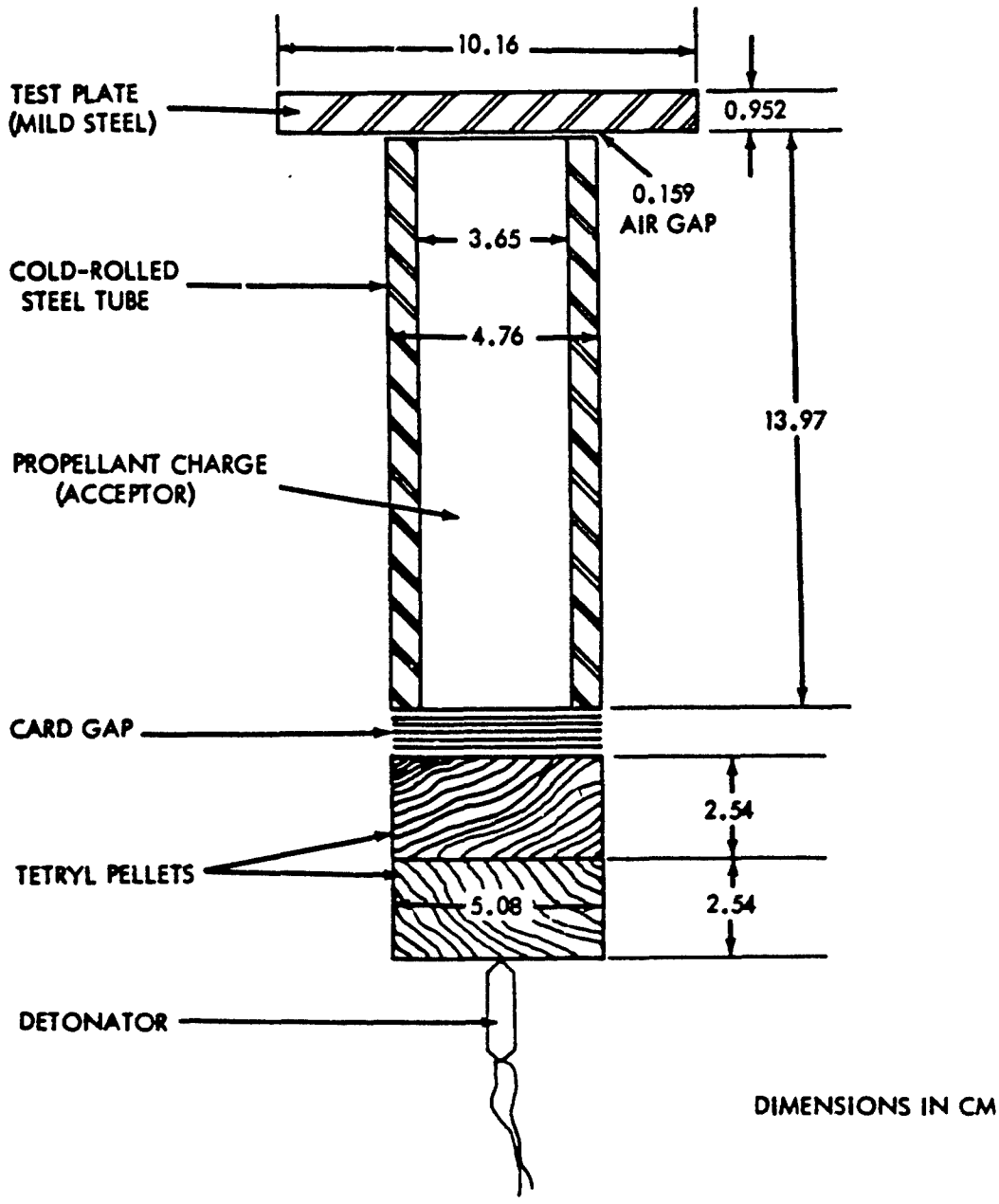


FIG. A1 CHARGE ASSEMBLY AND DIMENSIONS FOR NOL STANDARDIZED GAP TEST

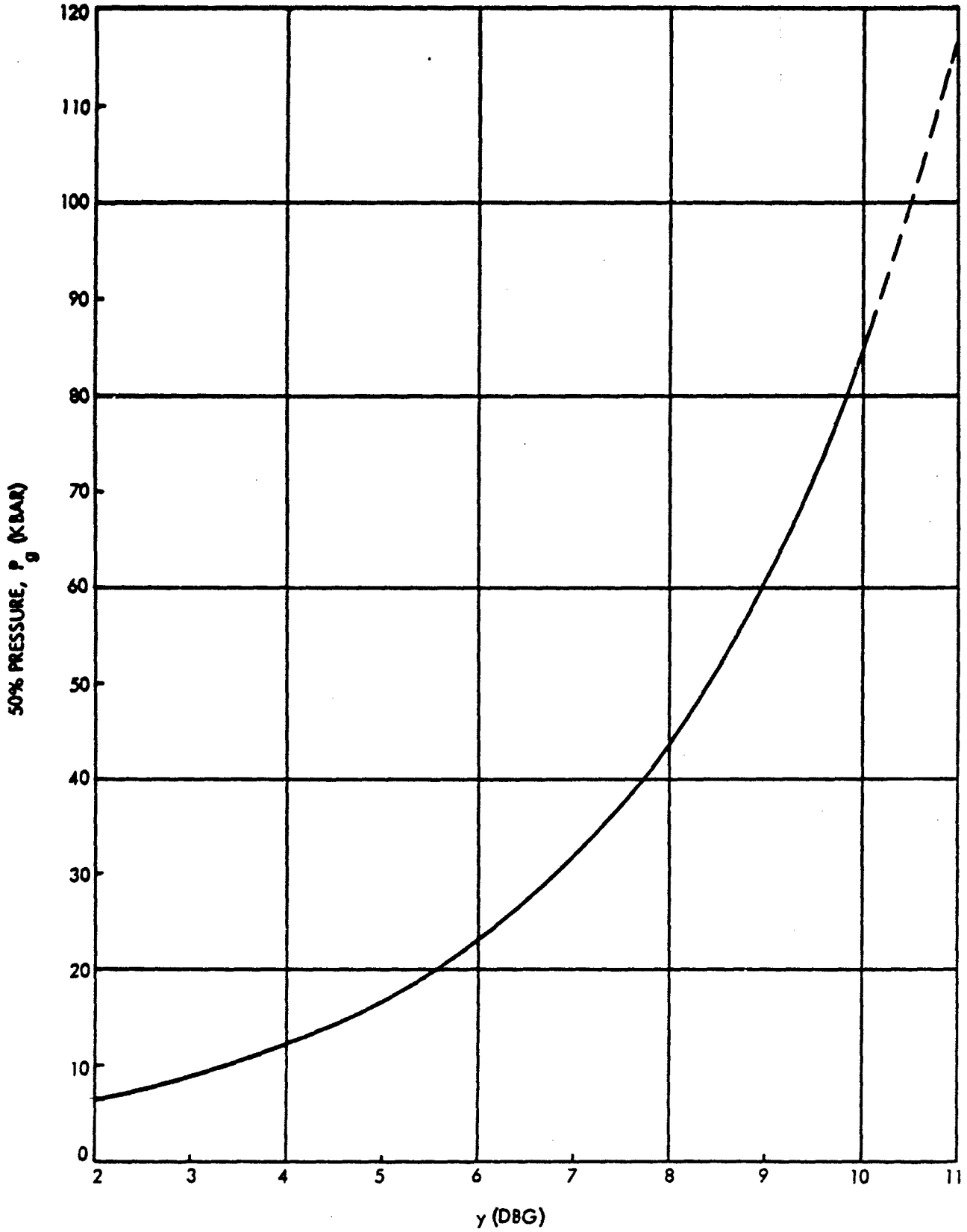


FIG. A2 CONVERSION SSGT RESULTS FROM ARBITRARY UNITS TO $P_g$ (KBAR)

Best Available Copy

# APPENDIX B

## MEASUREMENT OF SHOCK VELOCITY

Because the SSGT donor/gap system has such small dimensions, it is impossible to make accurate velocity measurements (with the smear camera) of the shock front moving through the barrier. However, instantaneous shock velocities were obtained in the usual manner[2] working with model systems 5x the actual size and a smear camera set at the writing speed of 1.9 mm/μsec.

The data of shock-velocity as a function of distance traveled in PMMA obtained in four shots of the SSGT calibration (shot nos. 222, 223, 242, and 243) are given in Table B1 and plotted in Fig. B1. The spread in U for each value of X indicates the extreme values of the four shots and the dot represents the mean value.

At given values of X, u and U are read from the curves in Figs. 5 and B1 respectively, u being 1/2 $u_{fs}$. If U is plotted against u, the curve of Fig. B2 is obtained. This curve is very similar to the dashed curve (from Fig. 6) which was derived in making the LSGT calibration. It is clear in both cases that U levels off as u approaches zero.

There are not as many shock-velocity data available from the SSGT calibration as from the LSGT calibration and the spread in the data is somewhat greater. Also, the blocks of PMMA used in making the SSGT shock-velocity measurements were 4-5 in. thick as compared to only 2 in. in the LSGT. The greater thickness makes it more difficult to pin-point the exact start of the smear-camera trace. A deviation (easily realized) of ± 1 mm from the actual start can cause an error of ± 2-3% in U between X=0 and X=25 mm (scale factor = 5). In spite of these difficulties the agreement is good between the u-U data obtained in the two calibrations.

TABLE B1

Shock velocity (U) as a function of the distance (X) the shock has travelled in PMMA for the SSGT. (X scale factor is five)

| X | U (mm/μsec) | | | | |
|---|---|---|---|---|---|
| (mm) | No. 222 | No. 223 | No. 242 | No. 243 | Mean |
| 0 | 6.71 | 6.96 | 6.92 | 7.02 | 6.90 |
| 5 | 6.00 | 5.89 | 6.19 | 6.58 | 6.17 |
| 10 | 5.24 | 5.36 | 5.52 | 5.70 | 5.46 |
| 15 | 4.64 | 4.84 | 4.90 | 4.96 | 4.84 |
| 20 | 4.18 | 4.39 | 4.38 | 4.47 | 4.36 |
| 25 | 3.84 | 3.97 | 3.91 | 4.04 | 3.94 |
| 30 | 3.59 | 3.64 | 3.60 | 3.75 | 3.65 |
| 35 | 3.38 | 3.44 | 3.35 | 3.35 | 3.38 |
| 40 | 3.27 | 3.33 | 3.27 | 3.33 | 3.30 |
| 50 | 3.14 | 3.18 | 3.16 | 3.23 | 3.18 |
| 60 | 3.07 | 3.13 | 3.10 | 3.18 | 3.12 |
| 70 | 3.07 | 3.10 | 3.06 | 3.13 | 3.09 |
| 80 | 3.07 | 3.06 | 3.06 | 3.13 | 3.08 |
| 90 | 3.03 | 3.04 | 3.06 | 3.13 | 3.07 |
| 100 | 3.00 | 3.02 | 3.00 | 3.06 | 3.02 |
| 110 | 2.96 | 3.02 | 3.00 | 3.04 | 3.01 |
| 120 | 2.96 | 3.02 | 2.97 | 3.04 | 3.00 |

Best Available Copy

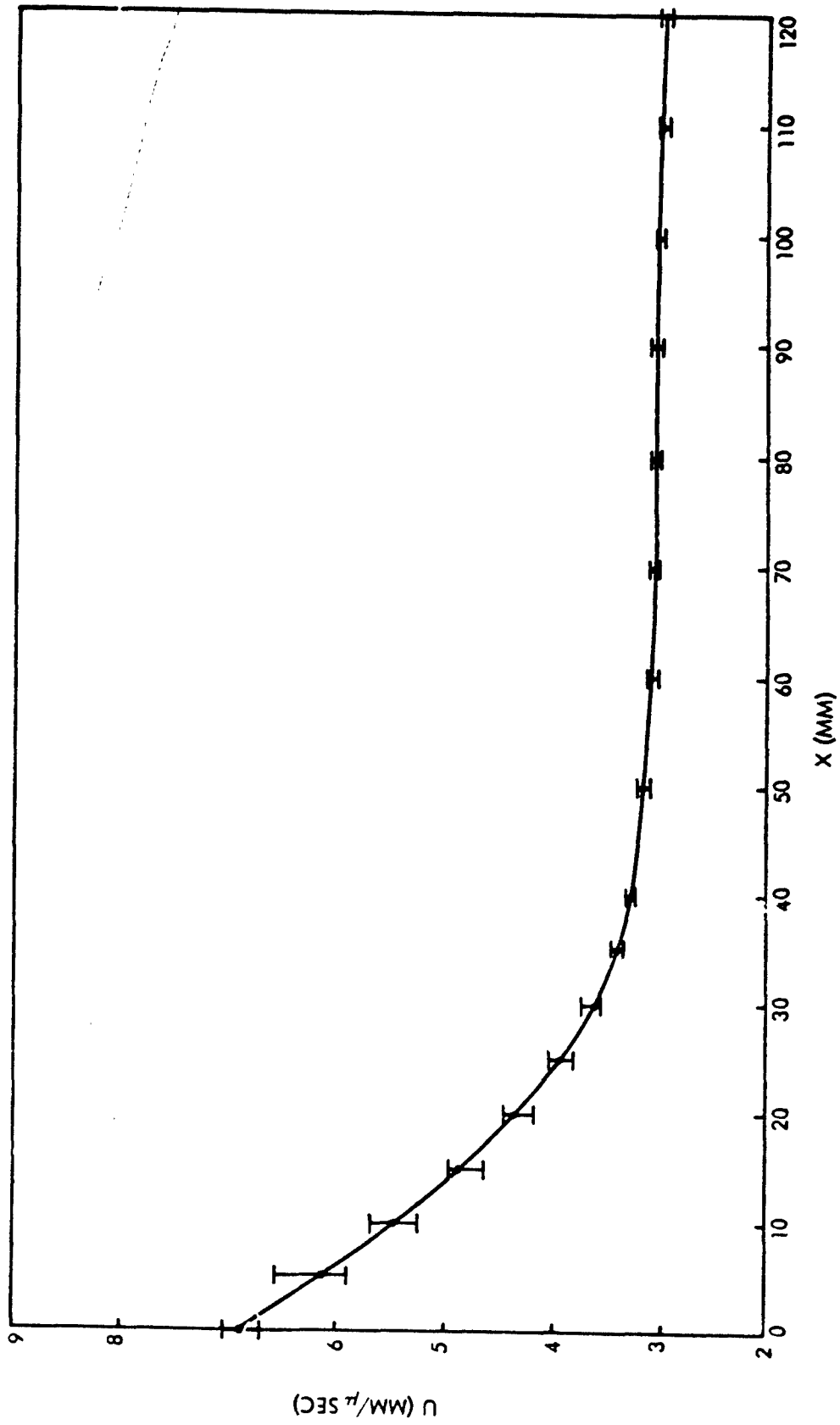


FIG. B1 SHOCK VELOCITY (U) VS DISTANCE (X) IN PMMA IN SSGT
(X SCALE FACTOR IS FIVE)

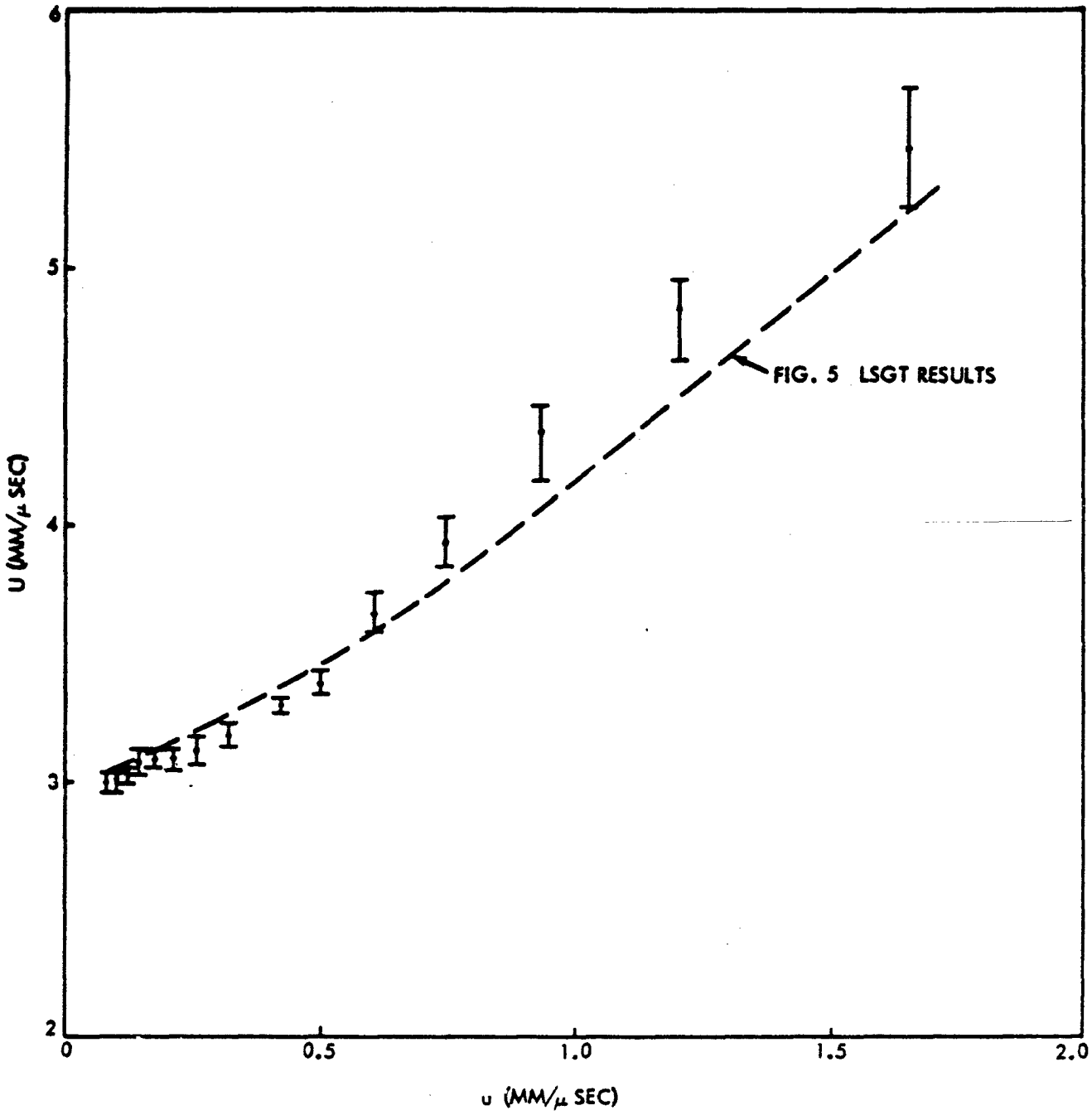


FIG. B2 PMMA HUGONIOT DATA OBTAINED IN CALIBRATION OF SSGT

Best Available Copy

UNCLASSIFIED
Security Classification

## DOCUMENT CONTROL DATA - R&D

(Security classification of title, body of abstract and indexing annotation must be entered when the overall report is classified)

1. ORIGINATING ACTIVITY (Corporate author)
U. S. Naval Ordnance Laboratory, White Oak
Silver Spring, Maryland 20910

2a. REPORT SECURITY CLASSIFICATION
UNCLASSIFIED

2b. GROUP --

3. REPORT TITLE
The Small Scale Gap Test: Calibration and Comparison with the Large Scale Gap Test

4. DESCRIPTIVE NOTES (Type of report and inclusive dates)

5. AUTHOR(S) (Last name, first name, initial)
PRICE, Donna; LIDDIARD, T. P. Jr.

6. REPORT DATE
7 July 1966

7a. TOTAL NO. OF PAGES
50

7b. NO. OF REFS
11

8a. CONTRACT OR GRANT NO.

b. PROJECT NO.
RMMP 22-149-F009-06-11 and
c. RMMO 62-058/212-1/F008-08-11

d.

9a. ORIGINATOR'S REPORT NUMBER(S)
NOLTR 66-87

9b. OTHER REPORT NO(S) (Any other numbers that may be assigned this report)

10. AVAILABILITY/LIMITATION NOTICES
This document is subject to special export controls and each transmittal to foreign governments or foreign nationals may be made only with prior approval of NOL.

11. SUPPLEMENTARY NOTES

12. SPONSORING MILITARY ACTIVITY
Bureau of Naval Weapons

13. ABSTRACT

The calibration of the small scale gap test (SSGT) is reported. It covers the ranges of 5 to 90 kbar in shock pressure and 2 to 20 mm in gap thickness of polymethyl methacrylate and can be simply extrapolated beyond these ranges.

Comparison of the shock sensitivities measured in the SSGT with those obtained in the large scale gap test showed quantitative correlation for explosives tested at porosity ≥ 10%. Differences at lower porosities are described and discussed.

DD FORM 1 JAN 64 1473

UNCLASSIFIED
Security Classification

Best Available Copy

UNCLASSIFIED
Security Classification

| 14 KEY WORDS | LINK A ROLE | LINK A WT | LINK B ROLE | LINK B WT | LINK C ROLE | LINK C WT |
|---|---|---|---|---|---|---|
| Shock Sensitivity | | | | | | |
| Calibration of Gap Test | | | | | | |
| Small Scale Gap Test | | | | | | |
| Large Scale Gap Test | | | | | | |

## INSTRUCTIONS

1. ORIGINATING ACTIVITY: Enter the name and address of the contractor, subcontractor, grantee, Department of Defense activity or other organization (*corporate author*) issuing the report.

2a. REPORT SECURITY CLASSIFICATION: Enter the overall security classification of the report. Indicate whether "Restricted Data" is included. Marking is to be in accordance with appropriate security regulations.

2b. GROUP: Automatic downgrading is specified in DoD Directive 5200.10 and Armed Forces Industrial Manual. Enter the group number. Also, when applicable, show that optional markings have been used for Group 3 and Group 4 as authorized.

3. REPORT TITLE: Enter the complete report title in all capital letters. Titles in all cases should be unclassified. If a meaningful title cannot be selected without classification, show title classification in all capitals in parenthesis immediately following the title.

4. DESCRIPTIVE NOTES: If appropriate, enter the type of report, e.g., interim, progress, summary, annual, or final. Give the inclusive dates when a specific reporting period is covered.

5. AUTHOR(S): Enter the name(s) of author(s) as shown on or in the report. Enter last name, first name, middle initial. If military, show rank and branch of service. The name of the principal author is an absolute minimum requirement.

6. REPORT DATE: Enter the date of the report as day, month, year, or month, year. If more than one date appears on the report, use date of publication.

7a. TOTAL NUMBER OF PAGES: The total page count should follow normal pagination procedures, i.e., enter the number of pages containing information.

7b. NUMBER OF REFERENCES: Enter the total number of references cited in the report.

8a. CONTRACT OR GRANT NUMBER: If appropriate, enter the applicable number of the contract or grant under which the report was written.

8b, 8c, & 8d. PROJECT NUMBER: Enter the appropriate military department identification, such as project number, subproject number, system numbers, task number, etc.

9a. ORIGINATOR'S REPORT NUMBER(S): Enter the official report number by which the document will be identified and controlled by the originating activity. This number must be unique to this report.

9b. OTHER REPORT NUMBER(S): If the report has been assigned any other report numbers (*either by the originator or by the sponsor*), also enter this number(s).

10. AVAILABILITY/LIMITATION NOTICES: Enter any limitations on further dissemination of the report, other than those imposed by security classification, using standard statements such as:

(1) "Qualified requesters may obtain copies of this report from DDC."

(2) "Foreign announcement and dissemination of this report by DDC is not authorized."

(3) "U. S. Government agencies may obtain copies of this report directly from DDC. Other qualified DDC users shall request through _____."

(4) "U. S. military agencies may obtain copies of this report directly from DDC. Other qualified users shall request through _____."

(5) "All distribution of this report is controlled. Qualified DDC users shall request through _____."

If the report has been furnished to the Office of Technical Services, Department of Commerce, for sale to the public, indicate this fact and enter the price, if known.

11. SUPPLEMENTARY NOTES: Use for additional explanatory notes.

12. SPONSORING MILITARY ACTIVITY: Enter the name of the departmental project office or laboratory sponsoring (*paying for*) the research and development. Include address.

13. ABSTRACT: Enter an abstract giving a brief and factual summary of the document indicative of the report, even though it may also appear elsewhere in the body of the technical report. If additional space is required, a continuation sheet shall be attached.

It is highly desirable that the abstract of classified reports be unclassified. Each paragraph of the abstract shall end with an indication of the military security classification of the information in the paragraph, represented as (*TS*), (*S*), (*C*), or (*U*).

There is no limitation on the length of the abstract. However, the suggested length is from 150 to 225 words.

14. KEY WORDS: Key words are technically meaningful terms or short phrases that characterize a report and may be used as index entries for cataloging the report. Key words must be selected so that no security classification is required. Identifiers, such as equipment model designation, trade name, military project code name, geographic location, may be used as key words but will be followed by an indication of technical context. The assignment of links, roles, and weights is optional.

UNCLASSIFIED
Security Classification